REPORT DOCUMENTATION PAGE

Form Approved
OMB No. 0704-0188

The public reporting burden for this collection of information is estimated to average 1 hour per response, including the time for reviewing instructions, searching existing data sources, gathering end maintaining the data needed, and completing and reviewing the collection of information. Send comments regarding this burden estimate or eny other aspect of this collection of informetion, including suggestions for reducing the burden, to the Department of Defense, Executive Service Directorate (0704-0188). Respondents should be aware thet notwithstanding eny other provision of lew, no person shall be subject to any penalty for failing to comply with a collection of information if it does not display a currently valid OMB control number.

PLEASE DO NOT RETURN YOUR FORM TO THE ABOVE ORGANIZATION.

1. REPORT DATE *(DD-MM-YYYY)*	2. REPORT TYPE	3. DATES COVERED *(From - To)*
11-30-2009		12/01/2007-08/31/2009

4. TITLE AND SUBTITLE
Flight Mechanics of Reversible Attachment Landing for Micro-Aerial Vehicles with Self-Decontaminating Surfaces

5a. CONTRACT NUMBER

5b. GRANT NUMBER
FA9550-08-1 ~~009~~ 0009

5c. PROGRAM ELEMENT NUMBER

6. AUTHOR(S)
T. M. Seigler

5d. PROJECT NUMBER

5e. TASK NUMBER

5f. WORK UNIT NUMBER

7. PERFORMING ORGANIZATION NAME(S) AND ADDRESS(ES)
University of Kentucky Research Foundation
201 Kinkead Hall
Lexington, KY 40506-0001
(859)257-9420

8. PERFORMING ORGANIZATION REPORT NUMBER

9. SPONSORING/MONITORING AGENCY NAME(S) AND ADDRESS(ES)
US Air Force Office of Scientific Research

10. SPONSOR/MONITOR'S ACRONYM(S)

11. SPONSOR/MONITOR'S REPORT NUMBER(S)
AFRL-SR-AR-TR-10-0119

12. DISTRIBUTION/AVAILABILITY STATEMENT
Distribution A; Approved for Public Release

20100316228

13. SUPPLEMENTARY NOTES

14. ABSTRACT
This work investigates the problem of landing on a vertical surface for flapping wing micro-aerial vehicles (MAV's) equipped with a self-decontaminating surface that allows attachment without a large force application. The analysis is based on time averaging theory which allows the wing motion and its resulting aerodynamic force to be characterized by parametric components of periodic functions. It is shown that a three-degree of freedom wing is required for the general maneuvering requirements of attachment landing. These kinematic variables are wing rotation, wing sweep, and variable frequency flapping speed. For the flight control problem, nonlinear methods of backstepping and and dynamic inversion are shown to be well-suited for achieving the necessary tracking commands.

15. SUBJECT TERMS

16. SECURITY CLASSIFICATION OF:			17. LIMITATION OF ABSTRACT	18. NUMBER OF PAGES	19a. NAME OF RESPONSIBLE PERSON
a. REPORT	b. ABSTRACT	c. THIS PAGE			19b. TELEPHONE NUMBER *(Include area code)*

Contents

1 Introduction and Overview.

This work investigates the attachment landing problem for flapping wing micro-aerial vehicles (MAV's). Landing is a critical operational component, necessary for conducting surveillance, and conserving/harvesting energy. Autonomous landing requirements for the MAV are quite different than for conventional aircraft as the MAV may be expected to identify its own set-down point while operating in highly constrained and unfamiliar surroundings. Recent advancements in surface adhesion technology offer to greatly enhance landing capabilities by allowing the MAV to attach to any nearby vertical surface, much like flying insects, and then detach with little effort. Researchers have recently attempted to design (Jagota and Bennisson, 2002; Glassmaker et al., 2004; Hui et al., 2004; Bhushan et al., 2006) and fabricate (Geim et al., 2003; Sitti, 2003; Sitti and Fearing, 2003; Northen and Turner, 2005; Yurdumakan, et al., 2005) these types of adhesives, also called bio-inspired tapes.

Biological studies have revealed that flying insects execute landing maneuvers ranging in complexity. For example, the honeybee utilizes a very simple control strategy when landing upright on a flat horizontal surface (Srinivasan et al., 2001). Alternatively, the housefly will land upside-down on a ceiling by extending its forward legs over its head, making contact, and then using momentum to rotate the remainder of its body 180-degrees to the ceiling (Borst, 1990). The particular landing strategy adopted by insects is dependent on various factors including inherent flight capabilities and "landing gear"; the honeybee is much more adept at hovering flight while the housefly has superior surface adhesion. The agility demonstrated by flying insects is difficult to mimic. The equations of motion for the flapping wing vehicle are naturally unstable (a key factor of agility) and contain substantial nonlinearities. The control problem has been recently investigated by relatively small number of researchers (Deng et al., 2006; Schenato, 2003; Schenato et al., 2003). The standard approach to control is based on time averaging theory (Sanders and Verhulst, 1985), which stems from the fact that the motion of the wings is substantially faster than the motion of the body to which they are attached.

The problem addressed by this work that of vertical attachment landing where, generally stated, the objective is to control the vehicle such that its attachment surface can make contact with a vertical surface. It is assumed that the contact surface is situated on the underbelly of the vehicle, so that the landing requires a relatively large pitch angle. The two primary questions addressed here are: (1) what are the actuation requirements to produce the required landing maneuver?; and (2) how can this maneuver be controlled?

The outline of this report is as follows. The equation of motion for a flapping wing vehicle are derived in Sec. 2, with the aim of generality. In Sec. 3, the longitudinal equations are considered with the objective of deriving general expressions for the actuation requirements of the vehicle. In this section, several critical assumptions as to the necessary wing degrees of freedom. Methods of nonlinear control are applied to the longitudinal dynamics in Sec. 4. Section 5 contains a numerical example of the theoretical development of the preceding sections, based on the planform properties of the bumblebee. Conclusions of this work are stated in Sec. 6.

2 Flight mechanics.

2.1 Kinematics.

The body is divided into three components: the main body, and the two wings. The main body kinematics are referenced to an inertial reference frame, denoted $\mathscr{R}_0$, as required by the kinetic equations. The motion of the wings are referenced to the main body reference frame, $\mathscr{R}_1$. The

notation followed throughout this section is explained in the Appendix (Sec. 6.1).

2.1.1 Main-body kinematics.

Let the position vector $\boldsymbol{R}$ locate a material point of the flight vehicle relative to an inertial reference frame; $[\boldsymbol{R}]_0$ is the $\mathscr{R}_0$-representation of this position vector. Let $\boldsymbol{R}_1$ locate the origin of a reference frame $\mathscr{R}_1$ that is attached to some rigid portion of the main body and confined to rotate and translate with it. A material point is located relative to $\mathscr{R}_1$ by the vector $\boldsymbol{R}'$ so that

$$\boldsymbol{R} = \boldsymbol{R}_1 + \boldsymbol{R}'. \tag{2.1}$$

The $\mathscr{R}_0$ frame representation of this relation is

$$[\boldsymbol{R}]_0 = [\boldsymbol{R}_1]_0 + [\boldsymbol{R}']_0 = [\boldsymbol{R}_1]_0 + C_{01}[\boldsymbol{R}']_1, \tag{2.2}$$

and time derivative is

$$D_t([\boldsymbol{R}]_0) = D_t([\boldsymbol{R}_1]_0) - C_{01}[\boldsymbol{R}']_1^*[\boldsymbol{\omega}_{1/0}]_1 + C_{01}D_t([\boldsymbol{R}']_1). \tag{2.3}$$

The second time derivative is

$$\begin{aligned} D_{tt}([\boldsymbol{R}]_0) &= D_{tt}([\boldsymbol{R}_1]_0) - C_{01}[\boldsymbol{\omega}_{1/0}]_1^*[\boldsymbol{R}']_1^*[\boldsymbol{\omega}_{1/0}]_i - C_{01}[\boldsymbol{R}']_1^*D_t([\boldsymbol{\omega}_{1/0}]_1) \\ &+ 2C_{01}[\boldsymbol{\omega}_{1/0}]_1^*D_t([\boldsymbol{R}']_1) + C_{01}D_{tt}([\boldsymbol{R}']_1). \end{aligned} \tag{2.4}$$

Define $v_1 = C_{10}D_t([\boldsymbol{R}_1]_0)$ so that

$$D_{tt}([\boldsymbol{R}_1]_0) = C_{01}D_t(v_1) + C_{01}[\boldsymbol{\omega}_{1/0}]_1^*v_1. \tag{2.5}$$

Also, let $\dot{v}_1 = D_t(v_1)$, $\omega_1 = [\boldsymbol{\omega}_{1/0}]_1$, $\tilde{\omega}_1 = [\boldsymbol{\omega}_{1/0}]_1^*$, $\dot{\omega}_1 = D_t(\omega_1)$, $R' = [\boldsymbol{R}']_1$, $\dot{R}' = D_t([\boldsymbol{R}']_1)$, and $\tilde{R}' = [\boldsymbol{R}']_1^*$, so that

$$C_{10}D_t([\boldsymbol{R}]_0) = v_1 - \tilde{R}'\omega_1 + \dot{R}' \tag{2.6}$$

$$C_{10}D_{tt}([\boldsymbol{R}]_0) = \dot{v}_1 + \tilde{\omega}_1 v_1 - \tilde{\omega}_1\tilde{R}'\omega_1 - \tilde{R}'\dot{\omega}_1 - 2\dot{\tilde{R}}'\omega_1 + \ddot{R}'. \tag{2.7}$$

These are the two expressions required to formulate the dynamic equations. They are expressed relative to a fixed body frame. However, since the aerodynamic forces are expressed relative to the direction of air flow, it is often convenient to express the dynamics relative to a frame that aligns with the air flow.

The body velocity is $\boldsymbol{V}_1 := d\boldsymbol{R}_1/dt$, hence $D_t([\boldsymbol{R}_1]_0) = C_{01}v_1$. For the circumstance that atmosphere is non-stationary (i.e., the presence of wind gusts and cross-flow), the wind velocity, denoted $\boldsymbol{V}_w$, is necessary for an accurate prediction of the aerodynamic forces. To accommodate this situation the flight equations can be constructed in terms of the relative velocity

$$\boldsymbol{V}_{1/w} = \boldsymbol{V}_1 - \boldsymbol{V}_w, \tag{2.8}$$

which is the negative of the total wind velocity. The component $\boldsymbol{V}_w$ is not a known quantity and thus flight control designs are based on the assumption that it is negligible. The $\mathscr{R}_0$-representation of the previous equation is

$$[\boldsymbol{V}_{1/w}]_0 = [\boldsymbol{V}_1]_0 - [\boldsymbol{V}_w]_0 = D_t([\boldsymbol{R}_1]_0) - [\boldsymbol{V}_w]_0 = C_{01}v_1 - [\boldsymbol{V}_w]_0.$$

If the disturbance term $\boldsymbol{V}_w$ is zero, then it is clear that $v_1 = C_{10}[\boldsymbol{V}_{1/w}]_0 = [\boldsymbol{V}_{1/w}]_1$.

The *relative wind-axis*, denoted $\bar{\mathscr{R}}_1$, is defined such that

$$C_{\bar{1}1}[\boldsymbol{V}_{1/w}]_1 = [V_{T_1} \quad 0 \quad 0]^T, \tag{2.9}$$

where $[\boldsymbol{V}_{1/w}]_1 = C_{10}[\boldsymbol{V}_{1/w}]_0$, $V_{T_1} := |[\boldsymbol{V}_{1/w}]_1|$, and $C_{\bar{1}1}$ is the basis transformation operator $\mathscr{R}_1 \to \bar{\mathscr{R}}_1$. The relative motion of $\mathscr{R}_1$ and $\bar{\mathscr{R}}_1$ results in the angular velocity vector $\boldsymbol{\omega}_{\bar{1}/1}$ which describe the relative angular motion of the reference frames.

Taking the time derivative of the relative velocity vector, $C_{01}[\boldsymbol{V}_{1/w}]_1$ results in

$$D_t([\boldsymbol{V}_{1/w}]_0) = C_{01}[\boldsymbol{\omega}_{1/0}]_1^*[\boldsymbol{V}_{1/w}]_1 + C_{01}D_t([\boldsymbol{V}_{1/w}]_1). \tag{2.10}$$

Since $D_t([\boldsymbol{V}_{1/w}]_0) = D_{tt}([\boldsymbol{R}_1]_0) - D_t([\boldsymbol{V}_w]_0)$, it follows that

$$\dot{v}_1 + \tilde{\omega}_1 v_1 - C_{10}D_t([\boldsymbol{V}_w]_0) = D_t([\boldsymbol{V}_{1/w}]_1) + \tilde{\omega}[\boldsymbol{V}_{1/w}]_1. \tag{2.11}$$

It is noted that

$$D_t(C_{\bar{1}1}[\boldsymbol{V}_{1/w}]_1) = -[\boldsymbol{\omega}_{\bar{1}/1}]_w^* C_{\bar{1}1}[\boldsymbol{V}_{1/w}]_1 + C_{\bar{1}1}D_t([\boldsymbol{V}_{1/w}]_1). \tag{2.12}$$

For no disturbance, $v = [\boldsymbol{V}_{1/w}]_1$ and $\dot{v}_1 = D_t([\boldsymbol{V}_{1/w}]_1)$; hence

$$C_{\bar{1}1}\dot{v}_1 = D_t(C_{\bar{1}1}[\boldsymbol{V}_{1/w}]_1) + [\boldsymbol{\omega}_{\bar{1}/1}]_{\bar{1}}^* C_{\bar{1}1}[\boldsymbol{V}_{1/w}]_1. \tag{2.13}$$

Since $C_{\bar{1}1}[\boldsymbol{V}_{1/w}]_1 = [V_{T_1} \quad 0 \quad 0]^T$, it follows that $D_t(C_{\bar{1}1}[\boldsymbol{V}_{1/w}]_1) = [\dot{V}_T \quad 0 \quad 0]^T$, and thus

$$C_{\bar{1}1}\dot{v}_1 = [\dot{V}_{T_1} \quad 0 \quad 0]^T + [\boldsymbol{\omega}_{\bar{1}/1}]_{\bar{1}}^*[V_{T_1} \quad 0 \quad 0]^T. \tag{2.14}$$

The wind-axis transformation is then

$$\begin{aligned} C_{\bar{1}1}(\dot{v}_1 + \tilde{\omega}_1 v_1) &= [\dot{V}_{T_1} \quad 0 \quad 0]^T + [\boldsymbol{\omega}_{\bar{1}/1}]_{\bar{1}}^*[V_{T_1} \quad 0 \quad 0]^T + C_{\bar{1}1}\tilde{\omega}_1 v_1 \\ &= [\dot{V}_{T_1} \quad 0 \quad 0]^T + [\boldsymbol{\omega}_{\bar{1}/1}]_{\bar{1}}^*[V_{T_1} \quad 0 \quad 0]^T + C_{\bar{1}1}\tilde{\omega}_1 C_{1\bar{1}}[V_{T_1} \quad 0 \quad 0]^T \\ &= \dot{v}_{\bar{1}} + \left([\boldsymbol{\omega}_{\bar{1}/1}]_{\bar{1}}^* + C_{\bar{1}1}\tilde{\omega}C_{1\bar{1}}\right) v_{\bar{1}} \end{aligned} \tag{2.15}$$

where the symbols $v_{\bar{1}}$ and $\dot{v}_{\bar{1}}$ are evident.

The basis transformation $\mathscr{R}_0 \to \mathscr{R}_1$ is parameterized by the rotation by the 3-2-1 set of Euler angles $\Theta_1 := [\phi_1 \ \theta_1 \ \psi_1]^T$. The transformation matrix is

$$C_{10} = \begin{bmatrix} c(\theta_1)c(\psi_1) & c(\theta_1)s(\psi_1) & -s(\theta_1) \\ -c(\phi_1)s(\psi_1) + s(\phi_1)s(\theta_1)c(\psi_1) & c(\phi_1)c(\psi_1) + s(\phi_1)s(\theta_1)s(\psi_1) & s(\phi_1)c(\theta_1) \\ s(\phi_1)s(\psi_1) + c(\phi_1)s(\theta_1)c(\psi_1) & -s(\phi_1)c(\psi_1) + c(\phi_1)s(\theta_1)s(\psi_1) & c(\phi_1)c(\theta_1) \end{bmatrix}. \tag{2.16}$$

The relationship between ω_1 and Θ_1 is then given by

$$\omega_1 = \begin{bmatrix} 1 & 0 & -\sin\theta_1 \\ 0 & \cos\phi_1 & \sin\phi_1\cos\theta_1 \\ 0 & -\sin\phi_1 & \cos\phi_1\cos\theta_1 \end{bmatrix} \dot{\Theta}_1. \tag{2.17}$$

The relative motion between $\mathscr{R}_1$ and $\bar{\mathscr{R}}_1$ is quantified by the 3-2-1 set of Euler angles $\gamma_1 = 0$, α_1 (angle of attack), and β_1 (sideslip angle), in which case the transformation matrix is

$$C_{\bar{1}1} = \begin{bmatrix} \cos\beta_1 & \sin\beta_1 & 0 \\ -\sin\beta_1 & \cos\beta_1 & 0 \\ 0 & 0 & 1 \end{bmatrix} \begin{bmatrix} \cos\alpha_1 & 0 & \sin\alpha_1 \\ 0 & 1 & 0 \\ -\sin\alpha_1 & 0 & \cos\alpha_1 \end{bmatrix}. \tag{2.18}$$

Let $\Gamma_1 = [\gamma_1 \ \alpha_1 \ \beta_1]$. The components of the $\bar{\mathscr{R}}_1$ representation of the relative angular velocity vector $\boldsymbol{\omega}_{\bar{1}/1}$ are related to the relative angles by

$$[\boldsymbol{\omega}_{\bar{1}/1}]_{\bar{1}} = \begin{bmatrix} 0 & -\sin\beta_1 & 0 \\ 0 & -\cos\beta_1 & 0 \\ 0 & 0 & 1 \end{bmatrix} \dot{\Gamma}_1. \tag{2.19}$$

2.1.2 Wing kinematics.

The wings, considered rigid, are attached to the main body. To quantify the motion of the right wing, two fixed reference frames are defined, $\mathscr{R}_2$ and $\mathscr{R}_3$ (cf. Fig. 1.). The origin of $\mathscr{R}_2$ is located at a wing-body connection point. The origin of $\mathscr{R}_3$ is located at the wings aerodynamic center of pressure. These two frames may be such that $\dot{C}_{23} = 0$, but $C_{23} \neq I$; that is, there is some initial offset between the reference frames. The x_2 and x_3 axes are directed along the chord of the wing, the y_2 and y_3 axes are directed along the span toward the right, and the z_2 and z_3 axes are tangent to the chord and span directions (following the right-hand rule). Let $\boldsymbol{V}_2$ and $\boldsymbol{V}_3$ denote the velocity at the origin of $\mathscr{R}_2$ and $\mathscr{R}_3$, respectively. For the left, wing the frames $\mathscr{R}_4$ and $\mathscr{R}_5$ are defined in an identical manner. Generally, $\boldsymbol{V}_i$ denotes the velocity of the origin of frame $\mathscr{R}_i$.

The orthogonal transformation matrices C_{21} and C_{41} quantify the orientation of $\mathscr{R}_2$ and $\mathscr{R}_4$, respectively, relative to $\mathscr{R}_1$. Again utilizing the 3-2-1 set of Euler angles, the transformation matrices are given by

$$C_{i1} = \begin{bmatrix} c(\theta_i')c(\psi_i') & c(\theta_i')s(\psi_i') & -s(\theta_i') \\ -c(\phi_i')s(\psi_i') + s(\phi_i')s(\theta_i')c(\psi_i') & c(\phi_i')c(\psi_i') + s(\phi_i')s(\theta_i')s(\psi_i') & s(\phi_i')c(\theta_i') \\ s(\phi_i')s(\psi_i') + c(\phi_i')s(\theta_i')c(\psi_i') & -s(\phi_i')c(\psi_i') + c(\phi_i')s(\theta_i')s(\psi_i') & c(\phi_i')c(\theta_i') \end{bmatrix}, \tag{2.20}$$

for $i = 2, 4$, where

$$\begin{aligned} \phi_i' &= \phi_i^0 + \phi_i \\ \theta_i' &= \theta_i^0 + \theta_i \\ \psi_i' &= \psi_i^0. \end{aligned}$$

Here ϕ_i^0, θ_i^0, ψ_i^0 are constants quantifying the initial offset. The angles ϕ_2 and ϕ_3 are called the *flapping angles.* The angles The angles θ_2 and θ_3 are called the *pronation angles.* Finally, ψ_2 and ψ_3 are called the *stroke angles.*

Let ϕ_3, θ_3, ψ_3 denote the constant offset parameters of C_{32}. The resulting transformation is

$$C_{32} = \begin{bmatrix} c(\theta_3)c(\psi_3) & c(\theta_3)s(\psi_3) & -s(\theta_3) \\ -c(\phi_3)s(\psi_3) + s(\phi_3)s(\theta_3)c(\psi_3) & c(\phi_3)c(\psi_3) + s(\phi_3)s(\theta_3)s(\psi_3) & s(\phi_3)c(\theta_3) \\ s(\phi_3)s(\psi_3) + c(\phi_3)s(\theta_3)c(\psi_3) & -s(\phi_3)c(\psi_3) + c(\phi_3)s(\theta_3)s(\psi_3) & c(\phi_3)c(\theta_3) \end{bmatrix}. \tag{2.21}$$

Similarly, for C_{54}:

$$C_{54} = \begin{bmatrix} c(\theta_5)c(\psi_5) & c(\theta_5)s(\psi_5) & -s(\theta_5) \\ -c(\phi_5)s(\psi_5) + s(\phi_5)s(\theta_5)c(\psi_5) & c(\phi_5)c(\psi_5) + s(\phi_5)s(\theta_5)s(\psi_5) & s(\phi_5)c(\theta_5) \\ s(\phi_5)s(\psi_5) + c(\phi_5)s(\theta_5)c(\psi_5) & -s(\phi_5)c(\psi_5) + c(\phi_5)s(\theta_5)s(\psi_5) & c(\phi_5)c(\theta_5) \end{bmatrix}. \tag{2.22}$$

The relative rotation rate of the reference frames is quantified by the vectors $\boldsymbol{\omega}_{2/1}$ and $\boldsymbol{\omega}_{4/1}$. Let $\omega_{i/1} = [\boldsymbol{\omega}_{i/1}]_i$ and $\Theta_{i/1} = [\phi_i' \ \theta_i' \ \psi_i']^T$ for $i = 2, 4$ so that

$$\omega_{i/1} = \begin{bmatrix} 1 & 0 & -\sin\theta_i' \\ 0 & \cos\phi_i' & \sin\phi_i'\cos\theta_i' \\ 0 & -\sin\phi_i' & \cos\phi_i'\cos\theta_i' \end{bmatrix} \dot{\Theta}_{i/1} = G_{i/1}\dot{\Theta}_{i/1}. \tag{2.23}$$

Define two additional reference frames $\bar{\mathscr{R}}_3$ and $\bar{\mathscr{R}}_5$, which indicate the relative orientation of the wind respect to the motion of the wings. The origins of these frames are coincident with $\mathscr{R}_3$ and $\mathscr{R}_5$.

The wing velocity relative to the wind is given by

$$\boldsymbol{V}_{i/w} = \boldsymbol{V}_i - \boldsymbol{V}_w, \quad i = 3, 5 \tag{2.24}$$

where $\boldsymbol{V}_{i/w}$ is the velocity of $\mathscr{R}_i$ relative to the airflow. Define $\bar{\mathscr{R}}_i$ $(i = 3, 5)$ such that

$$C_{\bar{i}i}[\boldsymbol{V}_{i/w}]_i = [V_{T_i}\ 0\ 0]^T, \quad i = 3, 5 \tag{2.25}$$

where $C_{\bar{3}3}$ and $C_{\bar{5}5}$ are, respectively, the basis transformation operators $\mathscr{R}_3 \to \bar{\mathscr{R}}_3$ and $\mathscr{R}_5 \to \bar{\mathscr{R}}_5$. These two transformations are parameterized by 3-2-1 Euler angles $\gamma_i = 0$, α_i and β_i; the latter two angles are the wing angle of attack and sideslip angle. The orthonormal transformations matrices are

$$C_{\bar{i}i} = \begin{bmatrix} -\sin\alpha_i' \cos\beta_i & -\sin\alpha_i' \sin\beta_i & \cos\alpha_i' \\ -\sin\beta_i & \cos\beta_i & 0 \\ -\cos\alpha_i' \cos\beta & \cos\alpha_i' \sin\beta & -\sin\alpha_i' \end{bmatrix}, \tag{2.26}$$

where $\alpha_i' = \pi/2 - \alpha$. The relative rotations of $\mathscr{R}_i$ and $\bar{\mathscr{R}}_i$ are quantified by the angular velocity vectors $\boldsymbol{\omega}_{\bar{3}/3}$ and $\boldsymbol{\omega}_{\bar{5}/5}$, with the relation

$$[\boldsymbol{\omega}_{\bar{i}/i}]_{\bar{i}} = \begin{bmatrix} 0 & -\sin\beta_i & 0 \\ 0 & -\cos\beta_i & 0 \\ 0 & 0 & 1 \end{bmatrix} \dot{\Gamma}_i, \tag{2.27}$$

where $\Gamma_i = [\gamma_i\ \alpha_i\ \beta_i]^T$, $i = 3, 5$.

2.2 Kinetics.

The equations of motion of an arbitrary nonpolar deformable body can be expressed in the general form

$$F^* - F - F' = 0, \tag{2.28}$$

where F^* the *generalized inertial force*, F the *generalized applied force*, and F' the *generalized constraint force*. Explicitly, these terms are

$$F^* = \int_{\mathcal{D}} \frac{\partial D_t([\mathbf{R}']_0)}{\partial y} \cdot D_{tt}([\mathbf{R}']_0)\, dm \tag{2.29}$$

$$F = \int_{\mathcal{D}} \frac{\partial D_t([\mathbf{R}']_0)}{\partial y} \cdot [\mathbf{b}]_0\, dm \tag{2.30}$$

$$F' = \int_{\mathcal{D}} \frac{\partial D_t([\mathbf{R}']_0)}{\partial y} \cdot [\mathbf{b}]_0\, dm, \tag{2.31}$$

where $\mathscr{R}_0$ is an inertial frame, y is an array of coordinates chosen to specify the motion of the body, $\mathcal{D}$ is the spatial volume of the body, and $\mathbf{b}$ and $\mathbf{b}'$ are, respectively, the applied and constraint force per unit mass. Constraint forces do not typically show up in flight analysis since the aircraft is a free body. However, they can be used to determine the internal actuation forces due to specified motions (i.e., morphing) of the aircraft.

When the main body is rigid, the kinematic parameters v_1 and ω_1 adequately quantify its motion. These kinematic parameters are regarded as *quasi-cordinates* since their integration does not yield any physically meaningful quantity. They are related to underlying kinematic quantities by

$$\begin{aligned} v_1 &= C_{10} D_t([\boldsymbol{R}_1]_0) \\ \omega_1 &= G_1 \dot{\Theta}_1. \end{aligned}$$

If the body is not rigid, additional coordinates are required to specify its motion. These additional coordinates can be treated in one of two ways: as additional states of the dynamical equations, or time-dependent extraneous inputs. For the analytical evaluation of complex structures, the latter approach is typically more useful. Mathematically, this amounts to the specification of *program constraints*, or *servoconstraints*, on certain kinematic parameters.

Likewise, the translational and rotational velocity of the (assumed rigid) wings are sufficient to describe their motion. Additionally, there must be constraint equations that couple the wing to the main body. However, a significant simplification ensues when the wings are considered massless. In this case, the generalized inertial force is dependent solely on main body motion, and also the generalized constraint force goes to zero. Defining the coordinate array

$$y = \begin{bmatrix} v_1 & \omega_1 \end{bmatrix}^T, \tag{2.32}$$

the generalized inertial force can be written

$$F_1^* = m\left(\dot{v} + \tilde{\omega} v\right) - S\dot{\omega} - \tilde{\omega} S \omega - 2\dot{S}\omega + \ddot{S} \tag{2.33}$$

$$F_2^* = S\left(\dot{v} + \tilde{\omega} v\right) + J\dot{\omega} + \tilde{\omega} J \omega + \dot{J}\omega + int_{\mathcal{D}} \tilde{p}\tilde{p}' \, dm \tag{2.34}$$

where $p = [\mathbf{R}']_1$, $F^* = [F_1^* \quad F_2^*]^T$, and

$$\begin{aligned} m &= \int_{\mathcal{D}} dm \\ S &= \int_{\mathcal{D}} \tilde{p} \, dm = \tilde{r}_c \\ J &= -\int_{\mathcal{D}} \tilde{p}\tilde{p} \, dm \end{aligned}$$

are, respectively, the mass and the first and second moments of inertia.

The matrix form (*i.e.*, reference frame dependent) of the translational and rotational equations of a morphing aircraft can be expressed in the form (Seigler et al., 2007)

$$m\dot{v} + m\tilde{\omega} v - m\tilde{r}_C \dot{\omega} - \tilde{\omega} m \tilde{r}_C \omega - 2m\dot{\tilde{r}}_C \omega + \ddot{r}_C = \mathcal{F} \tag{2.35}$$

$$m\tilde{r}_C \dot{v} + m\tilde{r}_C \tilde{\omega} v + J\dot{\omega} + \tilde{\omega} J \omega + \dot{J}\omega + int_{\mathcal{D}} \tilde{p}\ddot{p} \, dm = \mathcal{M} \tag{2.36}$$

where the components of the generalized applied force are $F = [\mathcal{F} \quad \mathcal{M}]^T$. The equations reduce to the standard rigid body flight equations when $\dot{p} = 0$ for every material point and the center of mass is chosen as the reference origin, requiring that $r_C = 0$. For the non-rigid case, it is also possible to let the body-fixed axis move with the center of mass, in which case again $r_C = 0$. However, v would then be the velocity of the center of mass rather than a "fixed" point of the vehicle. For sufficiently large aircraft speeds, this difference will have only a small effect. Note also that the moments of inertia may become more complicated when the reference point is in relative motion.

For the specified generalized velocities, the generalized applied forces are

$$\mathcal{F} = \int_{\mathcal{D}} [\mathbf{b}]_1 \, dm = [\mathbf{f}^a]_1 + [\mathbf{f}^g]_1 \tag{2.37}$$

$$\mathcal{M} = \int_{\mathcal{D}} \tilde{p}[\mathbf{b}]_1 \, dm = [\mathbf{m}^a]_1 + [\mathbf{m}^g]_1, \tag{2.38}$$

which are divided into aerodynamic and gravitational components. The gravitational force is given by

$$[\mathbf{f}^g]_1 = C_{10}[0 \; 0 \; mg]^T. \tag{2.39}$$

The moment due to gravity is

$$[\mathbf{m}^g]_1 = C_{10}\tilde{r}_C[0 \; 0 \; mg]^T. \tag{2.40}$$

A direct conversion of the inertial force to the wind axis results in

$$\begin{aligned} C_{\bar{1}1}F_1^* &= m\left\{\dot{v}_{\bar{1}} + \left([\boldsymbol{\omega}_{\bar{1}/1}]_{\bar{1}}^* + C_{\bar{1}1}\tilde{\omega}C_{1\bar{1}}\right)v_{\bar{1}}\right\} - C_{\bar{1}1}S\dot{\omega} - C_{\bar{1}1}\tilde{\omega}S\omega \\ &- 2C_{\bar{1}1}\dot{S}\omega + C_{\bar{1}1}\ddot{S} \end{aligned} \tag{2.41}$$

and

$$\begin{aligned} C_{\bar{1}1}F_2^* &= S\left\{\dot{v}_{\bar{1}} + \left([\boldsymbol{\omega}_{\bar{1}/1}]_w^* + C_{\bar{1}1}\tilde{\omega}C_{\bar{1}w}\right)v_{\bar{1}}\right\} + C_{\bar{1}1}J\dot{\omega} + C_{\bar{1}1}\left(\tilde{\omega}J + \dot{J}\right)\omega \\ &+ C_{\bar{1}1}int_{\mathcal{D}}\tilde{p}\ddot{p}\, d\mathcal{D} \end{aligned} \tag{2.42}$$

Thus, ignoring the presence of wind gusts and cross-flow etc., the equations of motion in the wind-axis become

$$m\dot{v}_{\bar{1}} + m\left(\tilde{\omega}_{\bar{1}/1} + C_{\bar{1}1}\tilde{\omega}C_{1\bar{1}}\right)v_{\bar{1}} - mC_{\bar{1}1}\tilde{r}_C\dot{\omega} - mC_{\bar{1}1}\tilde{\omega}\tilde{r}_C\omega - 2mC_{\bar{1}1}\dot{\tilde{r}}_C\omega + mC_{\bar{1}1}\ddot{r}_C = C_{\bar{1}1}\mathcal{F}$$

$$m\tilde{r}_C\dot{v}_{\bar{1}} + m\tilde{r}_C\left(\tilde{\omega}_{\bar{1}/1} + C_{\bar{1}1}\tilde{\omega}C_{1\bar{1}}\right)v_{\bar{1}} + C_{\bar{1}1}J\dot{\omega} + C_{\bar{1}1}\left(\tilde{\omega}J + \dot{J}\right)\omega + C_{\bar{1}1}\int_{\mathcal{D}}\tilde{p}\ddot{p}\, d\mathcal{D} = C_{\bar{1}1}\mathcal{M}.$$

2.3 Aerodynamic Forces

The aerodynamic force applied to a wing is quantified by

$$\mathbf{f}_i^a = \int_{S_i} \mathbf{t} \, dS_i, \quad i = 3, 5 \tag{2.43}$$

where $\mathbf{f}_i^a$ is resultant aerodynamic force applied at the origin of $\mathscr{R}_i$, located at the center of pressure, $\mathbf{t}$ is the traction force per unit area, and S_i denotes the external area of the wing. The moment of the aerodynamic force, about the center of mass of the vehicle, is

$$\mathbf{m}_i^a = \int_{S_i} \boldsymbol{R}_{i/1} \times \mathbf{t} \, dS, \tag{2.44}$$

where $\boldsymbol{R}_{\bar{i}/c}$ locates the origin of $\bar{\mathscr{R}}_i$, located at the center of pressure of the wing, with respect to $\mathscr{R}_1$.

The aerodynamic forces are considered to be functionally dependent on the instantaneous position of the wing and its velocity, both relative to the airflow. The aerodynamic force vector is divided into three components

$$\mathbf{f}^a = \mathbf{f}_1^a + \mathbf{f}_3^a + \mathbf{f}_5^a, \tag{2.45}$$

which denote, respectively, the force on the main body, the right wing, and the left wing (the indices correspond to the reference frame where the resultant force is applied). Further denote

$$[\mathbf{f}_1^a]_{\bar{1}} = [D_1\ 0\ L_1]^T \tag{2.46}$$
$$[\mathbf{f}_3^a]_{\bar{2}} = [D_3\ 0\ L_3]^T \tag{2.47}$$
$$[\mathbf{f}_5^a]_{\bar{3}} = [D_4\ 0\ L_5]^T \tag{2.48}$$

where L and D are the lift and drag forces. If it is reasonable to assume that the aerodynamic forces on the main body are small compared to the wings, which is the case for "slow flight", it can be assumed that $\mathbf{f}_a^1$ is negligible. The functional form of the lift and drag is expressed as

$$L_i = L_i(\alpha_i, \dot{\alpha}_i, \beta_i, \dot{\beta}_i, P_i, Q_i, V^{T_i}) \tag{2.49}$$
$$D_i = D_i(\alpha_i, \dot{\alpha}_i, \beta_i, \dot{\beta}_i, P_i, Q_i, V^{T_i}). \tag{2.50}$$

for $i = 3, 5$, where P_i and Q_i is a component of $[\boldsymbol{\omega}_{i/0}]_i = [P_i\ Q_i\ R_i]^T$.

Based on the published literature (Sane, 2003; Sane and Dickinson, 2001, 2002; Dickinson et al., 1993) regarding the aerodynamics of flapping wings, the instantaneous aerodynamic forces applied to the wings are composed of three distinct phenomena: *delayed stall*, *rotational lift*, and *wake capture*. Delayed stall contributes a significant majority of the aerodynamic force. Rotational lift and wake capture are due to the pronation of the wing, which typically occurs at the peaks of the up and down-stroke. Subsequent development is based on the assumption that wake capture is the predominant force, while rotational lift and wake capture are negligible. The wake capture component is represented by a force located at the center of pressure of the wing that is dependent on the instantaneous angle of attack, α_i, sideslip angle, β_i, and the relative wind velocity, V_{T_i}:

$$\mathbf{f}_i^a = \mathbf{f}_i^a(V_{T_i}, \alpha_i, \beta_i). \tag{2.51}$$

The corresponding moment is then

$$\mathbf{m}_i^a = \boldsymbol{R}_{\bar{i}/1} \times \mathbf{f}_i^a(V_{T_i}, \alpha_i, \beta_i).$$

Moreover, the force and moment are defined in the local wind axis; i.e.,

$$\begin{aligned}[\mathbf{m}_i^a]_{\bar{i}} &= [\boldsymbol{R}_{i/1} \times \mathbf{f}_i^a(V_{T_i}, \alpha_i, \beta_i)]_{\bar{i}} \\ &= [\boldsymbol{R}_{i/1}]_{\bar{i}}^* [\mathbf{f}_i^a(V_{T_i}, \alpha_i, \beta_i)]_{\bar{i}}.\end{aligned} \tag{2.52}$$

In the $\mathscr{R}_1$ frame, the moment is

$$[\mathbf{m}_i^a]_1 = C_{1i} C_{i\bar{i}} [\boldsymbol{R}_{i/1}]_{\bar{i}}^* [\mathbf{f}_i^a(V_{T_i}, \alpha_i, \beta_i)]_{\bar{i}}. \tag{2.53}$$

The position vector for the right wing is given by

$$\begin{aligned}[\boldsymbol{R}_{3/1}]_{\bar{3}} &= [\boldsymbol{R}_{2/1}]_{\bar{3}} + [\boldsymbol{R}_{3/2}]_{\bar{3}} \\ &= C_{\bar{3}3} C_{32} C_{21} [\boldsymbol{R}_{2/1}]_1 + C_{\bar{3}3} C_{32} [\boldsymbol{R}_{3/2}]_2\end{aligned}$$

where $[\boldsymbol{R}_{2/1}]_1$ and $[\boldsymbol{R}_{3/2}]_2$ are constants. Similarly, the position of the left wing is given by

$$[\boldsymbol{R}_{5/1}]_{\bar{5}} = C_{\bar{5}5} C_{41} [\boldsymbol{R}_{4/1}]_1 + C_{\bar{5}5} C_{54} [\boldsymbol{R}_{5/4}]_4 \tag{2.54}$$

where $[\boldsymbol{R}_{4/1}]_1$ and $[\boldsymbol{R}_{5/4}]_4$ are constants.

The aerodynamic force is dependent on the velocities of the wings, $\mathbf{V}_3$ and $\mathbf{V}_5$, which are given by

$$[\boldsymbol{V}_3]_3 = C_{31}\left[v_1 + \omega_1^*\left([\boldsymbol{R}_{2/1}]_1 + C_{12}[\boldsymbol{R}_{3/2}]_2\right)\right] + C_{32}[\boldsymbol{\omega}_{2/1}]_2^*[\boldsymbol{R}_{3/2}]_2 \tag{2.55}$$

$$[\boldsymbol{V}_5]_5 = C_{51}\left[v_1 + \omega_1^*\left([\boldsymbol{R}_{4/1}]_1 + C_{14}[\boldsymbol{R}_{5/4}]_4\right)\right] + C_{54}[\boldsymbol{\omega}_{4/1}]_4^*[\boldsymbol{R}_{5/4}]_4. \tag{2.56}$$

When the main body is stationary, or else if the first term of the summation is much less than the second (i.e., the body velocity is slow relative to the wing velocity), this reduces to

$$[\boldsymbol{V}_3]_3 = C_{32}[\boldsymbol{\omega}_{2/1}]_2^*[\boldsymbol{R}_{3/2}]_2 \tag{2.57}$$

$$[\boldsymbol{V}_5]_5 = C_{54}[\boldsymbol{\omega}_{4/1}]_4^*[\boldsymbol{R}_{5/4}]_4. \tag{2.58}$$

The velocities on which the aerodynamic force depends is now determined by

$$\begin{bmatrix} V_{T_i} \\ 0 \\ 0 \end{bmatrix} = C_{\bar{i}i}[\boldsymbol{V}_i]_i, \quad i = 3, 5. \tag{2.59}$$

Assuming that $[\boldsymbol{V}_i]_i$ is known, this constitutes three equations with three unknowns: α_i, β_i, V_{T_i}.

3 Actuation requirements.

In this section are methods of determining the actuation requirements of attachment landing, without consideration of feedback control. Also introduced in this section are several key simplifying assumptions that are necessary to achieve analytically tractable results.

3.1 Aerodynamic forces in "slow" flight.

When the flight speed of the vehicle is "slow", it is reasonable to assume that $v_1 = \omega_1 = 0$; and thus Eq. (2.59) reduces to

$$\begin{bmatrix} V_{T_3} \\ 0 \\ 0 \end{bmatrix} = C_{\bar{3}3}C_{32}[\boldsymbol{\omega}_{2/1}]_2^*[\boldsymbol{R}_{3/2}]_2 = \begin{bmatrix} \sin\alpha_3'\cos\beta_3\sin\theta_3 + \cos\alpha_3'\cos\theta_3 \\ \sin\beta_3\sin\theta_3 \\ \cos\alpha_3'\cos\beta_3\sin\theta_3 - \sin\alpha_3'\cos\theta_3 \end{bmatrix} y_{3/2}\dot{\phi}_2.$$

It follows that

$$\begin{aligned} \alpha_3 &= \theta_3 + \pi/2 \\ \beta_3 &= 0 \\ V_{T_3} &= y_{3/2}\dot{\phi}_2. \end{aligned}$$

Similarly, for the left wing

$$\begin{aligned} \alpha_5 &= \theta_5 + \pi/2 \\ \beta_5 &= 0 \\ V_{T_5} &= y_{5/4}\dot{\phi}_4. \end{aligned}$$

According to Dickenson et. al (1999), the magnitude of the aerodynamic force can be accurately quantified by

$$L_i(V_{T_i}, \alpha_i) = -\frac{1}{2}\rho S_i V_{T_i}^2 C_i \sin\alpha_i, \quad i = 3, 5, \tag{3.1}$$

where $\alpha_i \in [0, \pi/2]$, and C_i is a positive constant (a value of 3.5 was determined empirically by Dickenson et. al, 1999). For "slow" flight, this results in

$$L_3(V_{T_3}, \alpha_3) = \frac{1}{2}\rho S_3 (y_{3/2}\dot{\phi}_2)^2 C_3 \sin(\theta_3 + \pi/2) \tag{3.2}$$

$$L_5(V_{T_5}, \alpha_5) = \frac{1}{2}\rho S_5 (y_{5/4}\dot{\phi}_4)^2 C_5 \sin(\theta_5 + \pi/2). \tag{3.3}$$

Note that the lift is in the direction opposite of the wing motion. Expressed in the $\mathscr{R}_1$ frame, the aerodynamic forces are

$$\begin{aligned}[\mathbf{f}^a]_1 &= C_{1\bar{3}}[\mathbf{f}_3^a]_{\bar{3}} + C_{1\bar{5}}[\mathbf{f}_5^a]_{\bar{5}} \\ &= C_{12}C_{23}C_{3\bar{3}}[\mathbf{f}_3^a]_{\bar{3}} + C_{14}C_{45}C_{5\bar{5}}[\mathbf{f}_5^a]_{\bar{5}}\end{aligned} \tag{3.4}$$

The forces are dependent solely on the motion of the wings relative to the body.

The aerodynamic moment due to the force is found by

$$[\mathbf{m}_3^a]_1 = [\boldsymbol{R}_{3/1}]_1^*[\mathbf{f}_3^a]_1, \tag{3.5}$$

where

$$[\boldsymbol{R}_{3/1}]_1^* = [\boldsymbol{R}_{2/1}]_1 + C_{12}[\boldsymbol{R}_{3/2}]_2. \tag{3.6}$$

3.2 Method of averaging.

If the forces and moments produced by the wings occur periodically, and at a time scale much less than the motion of the vehicle body, the method of averaging can be used to produce a substantially simplified dynamic model. To show this, consider a periodic dynamical system of the form

$$\dot{\mathbf{x}} = \boldsymbol{f}(\mathbf{x}, t), \tag{3.7}$$

where

$$\boldsymbol{f}(\mathbf{x}, t) = \boldsymbol{f}(\mathbf{x}, t + T)$$

for some constant $T > 0$. The corresponding average systems is

$$\mathbf{x}_{avg}(t) = \frac{1}{T}\int_0^T \boldsymbol{f}\, dt. \tag{3.8}$$

With a change of timescale, i.e., $t = \tau T$, Eq. (X) can be written

$$\frac{d\mathbf{x}}{d\tau} = T\boldsymbol{f}(\boldsymbol{x}, \tau T), \tag{3.9}$$

and thus

$$\frac{d\mathbf{x}_{avg}}{d\tau} = T\boldsymbol{f}(\mathbf{x}_{avg}). \tag{3.10}$$

It is desired to approximate the dynamical system of Eq. (3.13) with that of the corresponding averaged system, Eq. (3.14). The theory of averaging (see e.g., Sec. 10.4 of Khalil, 2002) states that if T is sufficiently small then $\mathbf{x}(t) - \mathbf{x}_{avg}(t) = O(T)$, where O denotes the order of the error. Hence, the difference between the output of a dynamical system and its averaged output is small when the periodic frequency is large. This result can be extended to the case where the system contains a state-dependent control input; i.e., $\dot{\mathbf{x}} = \boldsymbol{f}(\mathbf{x}, \mathbf{u}(\mathbf{x}), t)$ (Schenato et. al., 2003).

Since the wing motion of a flapping wing vehicle is generally much faster than the gross motion of the vehicle, the method of averaging is assumed applicable. All subsequent theoretical development is based on this assumption. Its validity will be examined in the numerical example of Sec. 5.

3.3 Average forces and moments.

The wing motion is separated into the down-stroke and the up-stroke. The down-stroke is assumed to take place over a period T_1 seconds, and the up-stroke over a period of T_2 seconds; the total period is $T = T_1 + T_2$. During downstroke and upstroke, the ϕ_2 traverses the same angular range, A_ϕ, at an assumed constant angular velocity. The downstroke and upstroke angular velocity magnitudes are denoted $\dot{\phi}_2^d$ and $\dot{\phi}_2^u$ (both are positive valued). The periods, amplitude, and angular velocities are related by

$$T_1 = \frac{A_\phi}{\dot{\phi}_2^d}, \quad T_2 = \frac{A_\phi}{\dot{\phi}_2^u}. \tag{3.11}$$

Let f_ϕ denote the flapping frequency, which is related by

$$A_\phi f_\phi = \frac{\dot{\phi}_2^d \dot{\phi}_2^u}{\dot{\phi}_2^d + \dot{\phi}_2^u} \tag{3.12}$$

On the down stroke, let $\theta_3 = -\pi/4$ so that $\alpha_3' = \pi/4$; it follows that

$$C_{12}C_{23}C_{3\bar{3}} = C_{12} \begin{bmatrix} -1 & 0 & 0 \\ 0 & 1 & 0 \\ 0 & 0 & -1 \end{bmatrix}.$$

The force on the down-stroke is thus

$$[\mathbf{f}_3^a]_1 = -\frac{1}{2}\rho S_3 (y_{3/2}\dot{\phi}_2)^2 C \sin(\theta_3 + \pi/2) \begin{bmatrix} s\phi_2 s\psi_2 + c\phi_2 s\theta_2 c\psi_2 \\ -s\phi_2 c\psi_2 + c\phi_2 s\theta_2 s\psi_2 \\ c\phi_2 c\theta_2 \end{bmatrix} \tag{3.13}$$

On the upstroke, let $\theta_3 = \pi/4$ so that $\alpha_3' = -\pi/4$; it follows that

$$C_{12}C_{23}C_{3\bar{3}} = C_{12} \begin{bmatrix} 1 & 0 & 0 \\ 0 & 1 & 0 \\ 0 & 0 & 1 \end{bmatrix}.$$

The force on the up-stroke is thus

$$[\mathbf{f}_3^a]_1 = \frac{1}{2}\rho S_3 (y_{3/2}\dot{\phi}_2)^2 C \sin(\theta_3 + \pi/2) \begin{bmatrix} s\phi_2 s\psi_2 + c\phi_2 s\theta_2 c\psi_2 \\ -s\phi_2 c\psi_2 + c\phi_2 s\theta_2 s\psi_2 \\ c\phi_2 c\theta_2 \end{bmatrix}. \tag{3.14}$$

Focusing on the down-stroke, the angle ψ_2 is taken to be constant, and $\theta_2 = 0$. Thus, ϕ_2 is the only non-constant.

The average force on the down-stroke is

$$-\frac{q}{2T_1} \begin{bmatrix} s\psi_2^d \int_0^{T_1} s\phi_2 \, dt + s\theta_2 c\psi_2^d \int_0^{T_1} c\phi_2 \, dt \\ -c\psi_2^d \int_0^{T_1} s\phi_2^d \, dt + s\theta_2 s\psi_2^d \int_0^{T_1} c\phi_2^d \, dt \\ c\theta_2 \int_0^{T_1} c\phi_2^d \, dt \end{bmatrix}$$

where

$$q = \frac{\sqrt{2}}{2}\rho S_3 (y_{3/2}\dot{\phi}_2)^2 C. \tag{3.15}$$

Similarly, the average up-stroke force is

$$\frac{q}{2T_2}\begin{bmatrix} s\psi_2^u \int_{T_1}^T s\phi_2\, dt + s\theta_2 c\psi_2^u \int_{T_1}^T c\phi_2\, dt \\ -c\psi_2^u \int_{T_1}^T s\phi_2^u\, dt + s\theta_2 s\psi_2^u \int_{T_1}^T c\phi_2^u\, dt \\ c\theta_2 \int_{T_1}^T c\phi_2^u\, dt \end{bmatrix}.$$

The average force over a cycle is found by

$$-\frac{q}{2T}\left(\begin{bmatrix} s\psi_2^d \int_0^{T_1} s\phi_2\, dt + s\theta_2 c\psi_2^d \int_0^{T_1} c\phi_2\, dt \\ -c\psi_2^d \int_0^{T_1} s\phi_2^d\, dt + s\theta_2 s\psi_2^d \int_0^{T_1} c\phi_2^d\, dt \\ c\theta_2 \int_0^{T_1} c\phi_2^d\, dt \end{bmatrix} + \begin{bmatrix} s\psi_2^u \int_{T_1}^T s\phi_2\, dt + s\theta_2 c\psi_2^u \int_{T_1}^T c\phi_2\, dt \\ -c\psi_2^u \int_{T_1}^T s\phi_2^u\, dt + s\theta_2 s\psi_2^u \int_{T_1}^T c\phi_2^u\, dt \\ c\theta_2 \int_{T_1}^T c\phi_2^u\, dt \end{bmatrix}\right)$$

Let $[\mathbf{f}^a]_1 = (\mathcal{F}_x, \mathcal{F}_y, \mathcal{F}_z)$, and denote the averaged version of these forces $(\mathcal{F}_x^a, \mathcal{F}_y^a, \mathcal{F}_z^a)$. Since the focus here is on the longitudinal equations, only $\mathcal{F}_x^a$ and $\mathcal{F}_z^a$ are of interest. Assuming $\psi_2^d = \psi_2^u$, these average forces are

$$\mathcal{F}_x^a = -\frac{q}{T}\sin(A_{\phi/2})\sin\theta_2\cos\psi_2(\dot{\phi}_2^d - \dot{\phi}_2^u) \tag{3.16}$$

$$\mathcal{F}_z^a = -\frac{q}{T}\sin(A_{\phi/2})\cos\theta_2(\dot{\phi}_2^d - \dot{\phi}_2^u). \tag{3.17}$$

To determine the aerodynamic moment due to the force, assume that $[\boldsymbol{R}_{2/1}]_1 = [x_{2/1}\ y_{2/1}\ 0]^T$, so that

$$[\boldsymbol{R}_{3/1}]_1 = \begin{bmatrix} x_{2/1} \\ y_{2/1} \\ 0 \end{bmatrix} + \begin{bmatrix} -c\phi_2 s\psi_2 + s\phi_2 s\theta_2 c\psi_2 \\ c\phi_2 c\psi_2 + s\phi_2 s\theta_2 s\psi_2 \\ s\phi_2 c\theta_2 \end{bmatrix} y_{3/2}.$$

On the down-stroke the aerodynamic moment is

$$[\mathbf{m}_3^a]_1 = -\frac{\sqrt{2}}{4}\rho S_3(y_{3/2}\dot{\phi}_2)^2 C \begin{bmatrix} c\psi_2^d y_{3/2} + c\phi_2 y_{2/1} \\ s\psi_2^d y_{3/2} - x_{2/1}c\phi_2 \\ -s\phi_2(s\psi_2^d y_{2/1} + c\psi_2^d x_{2/1}) \end{bmatrix}, \tag{3.18}$$

and on the up-stroke the moment is

$$[\mathbf{m}_3^a]_1 = -\frac{\sqrt{2}}{4}\rho S_3(y_{3/2}\dot{\phi}_2)^2 C \begin{bmatrix} c\psi_2^u y_{3/2} + c\phi_2 y_{2/1} \\ s\psi_2^u y_{3/2} - x_{2/1}c\phi_2 \\ -s\phi_2(s\psi_2^u y_{2/1} + c\psi_2^u x_{2/1}) \end{bmatrix}. \tag{3.19}$$

Let $[\mathbf{m}_3^a]_1 = (\mathcal{M}_x, \mathcal{M}_y, \mathcal{M}_x)$, and denote the averaged version of these forces $(\mathcal{M}_x^a, \mathcal{M}_y^a, \mathcal{M}_x^a)$. For the longitudinal dynamics, only $\mathcal{M}_y^a$ is required, which is

$$\mathcal{M}_y^a = \frac{q}{T}\left(x_{2/1}\sin(A_\phi/2) - y_{3/2}A_\phi\sin\psi_2\right)\cos\theta_2(\dot{\phi}_2^d - \dot{\phi}_2^u). \tag{3.20}$$

The average forces and moments thus far calculated are for a single wing. When the wing motion is symmetric, these forces and moments are simply doubled in magnitude. That is, for symmetric wing motion, the total average forces and moments are

$$\mathcal{F}_x^a = -\frac{2q}{T}\sin(A_{\phi/2})\sin\theta_2\cos\psi_2(\dot{\phi}_2^d - \dot{\phi}_2^u) \tag{3.21}$$

$$\mathcal{F}_z^a = -\frac{2q}{T}\sin(A_{\phi/2})\cos\theta_2(\dot{\phi}_2^d - \dot{\phi}_2^u) \tag{3.22}$$

$$\mathcal{M}_y^a = \frac{2q}{T}\left(x_{2/1}\sin(A_\phi/2) - y_{3/2}A_\phi\sin\psi_2\right)\cos\theta_2(\dot{\phi}_2^d - \dot{\phi}_2^u). \tag{3.23}$$

or

$$\mathcal{F}_x^a = -2qf_\phi \sin(A_{\phi/2}) \sin\theta_2 \cos\psi_2(\dot{\phi}_2^d - \dot{\phi}_2^u) \tag{3.24}$$

$$\mathcal{F}_z^a = -2qf_\phi \sin(A_{\phi/2}) \cos\theta_2(\dot{\phi}_2^d - \dot{\phi}_2^u) \tag{3.25}$$

$$\mathcal{M}_y^a = 2qf_\phi \left(x_{2/1} \sin(A_\phi/2) - y_{3/2} A_\phi \sin\psi_2\right) \cos\theta_2(\dot{\phi}_2^d - \dot{\phi}_2^u). \tag{3.26}$$

The available control inputs are: θ_2, ψ_2, $\dot{\phi}_2^d$, and $\dot{\phi}_2^u$.

3.4 Longitudinal dynamics.

Assuming the main body is rigid, then with the standard longitudinal assumptions ($V = P = R = 0$) (Stevens and Lewis, 2003) the longitudinal dynamics are

$$m\dot{U} = -WQ - mg\sin\theta_1 + \mathcal{F}_x \tag{3.27}$$

$$m\dot{W} = UQ + mg\cos\theta_1 + \mathcal{F}_z \tag{3.28}$$

$$I_y\dot{Q} = \mathcal{M}_y. \tag{3.29}$$

The average dynamics are achieved by replacing $(\mathcal{F}_x, \mathcal{F}_z, \mathcal{M}_y)$ with their cyclic averages $(\mathcal{F}_x^a, \mathcal{F}_z^a, \mathcal{M}_y^a)$.

The steady-state dynamics are determined by

$$0 = -WQ - mg\sin\theta_1 - 2qf_\phi \sin(A_{\phi/2}) \sin\theta_2 \cos\psi_2(\dot{\phi}_2^d - \dot{\phi}_2^u) \tag{3.30}$$

$$0 = UQ + mg\cos\theta_1 - 2qf_\phi \sin(A_{\phi/2}) \cos\theta_2(\dot{\phi}_2^d - \dot{\phi}_2^u) \tag{3.31}$$

$$0 = 2qf_\phi \left(x_{2/1} \sin(A_\phi/2) - y_{3/2} A_\phi \sin\psi_2\right) \cos\theta_2(\dot{\phi}_2^d - \dot{\phi}_2^u). \tag{3.32}$$

For any given steady values θ_1, U, W, Q the equilibrium control inputs are

$$\psi_2 = \sin^{-1}\left(\frac{2x_{2/1}\sin(A_\phi/2)}{A_\phi y_{3/2}}\right) \tag{3.33}$$

$$\theta_2 = \tan^{-1}\left(\frac{WQ + mg\sin\theta_1}{-UQ - mg\cos\theta_1\cos\psi_2}\right) \tag{3.34}$$

$$\Phi_w = -\frac{-UQ - mg\cos\theta_1}{2qf_\phi \sin(A_\phi/2)\cos\theta_2}, \tag{3.35}$$

To determine a unique set of control inputs, it is assumed that the flapping frequency, f_ϕ, and amplitude, A_ϕ, is kept constant. From this specification, it follows that

$$A_\phi f_\phi \dot{\phi}_2^d - \dot{\phi}_2^d\dot{\phi}_2^u + A_\phi f_\phi \dot{\phi}_2^u = 0. \tag{3.36}$$

Since both $\dot{\phi}_2^d$ and $\dot{\phi}_2^u$ are positive valued, it must be that $\dot{\phi}_2^u > A_\phi f_\phi$; for simplicity, denote

$$\Phi_w := \dot{\phi}_2^d - \dot{\phi}_2^u. \tag{3.37}$$

An important subset of steady-state flight is the hovering mode where $U = W = Q = 0$. For a given pitch angle, θ_1, the steady actuation requirements are given by

$$\theta_2 = \tan^{-1}\left(\frac{-\tan\theta_1}{\cos\psi_2}\right) \tag{3.38}$$

$$\psi_2 = \sin^{-1}\left(\frac{2x_{2/1}\sin(A_\phi/2)}{A_\phi y_{3/2}}\right) \tag{3.39}$$

$$\Phi_w = \frac{mg\cos\theta_1}{2qf_\phi \sin(A_\phi/2)\cos\theta_2}, \tag{3.40}$$

where apparently ψ_2 and θ_2 must be non-zero.

3.5 Optimal landing trajectories.

The purpose of this section is to determine a trajectory that takes the vehicle body from one point to another, with the stipulation that the ending velocity is zero. The ending point is considered fixed; but the initial conditions, the trajectory, and the duration are all open for analysis. There are obviously infinite number of trajectories that take the vehicle from point A to point B while meeting the stipulated requirements. However, generally speaking, this should be accomplished with as little "effort" as possible. This consideration leads to optimization problems, the solution of which will specify both trajectories and, as a result, the forcing requirements.

Optimal trajectories are derived based on the planar inertial equations

$$F_x = m\ddot{x} \tag{3.41}$$

$$F_z - mg = m\ddot{z} \tag{3.42}$$

$$M_y = I_y\ddot{\theta}_1 \tag{3.43}$$

where $(x, -y, -z) = [\boldsymbol{R}_1]_0$, $(F_x, F_y, F_z) = [\mathbf{f}^a]_0$, and $(M_x, -M_y, -M_z) = [\mathbf{m}^a]_0$. The forces F_x, F_z, and moment, M_y are inertial representations. The conversions are $[\mathbf{f}^a]_1 = C_{10}[\mathbf{f}^a]_0$ and $[\mathbf{m}^a]_1 = C_{10}[\mathbf{m}^a]_0$. Given the longitudinal assumptions, the relationships are given by

$$\mathcal{F}_x = F_x \cos\theta - F_z \sin\theta \tag{3.44}$$

$$\mathcal{F}_z = -F_x \sin\theta - F_z \cos\theta \tag{3.45}$$

$$\mathcal{M}_y = -M_y. \tag{3.46}$$

The objective is to determine the trajectory $x(t)$, $y(t)$, and $\theta(t)$, subject to $\dot{x}(t_f) = \dot{y}(t_f) = \dot{\theta}(t_f) = 0$, that minimizes a specified performance index. Extremum of a prescribed functional

$$J = \int_0^t \mathbf{g}(\mathbf{x}, \dot{\mathbf{x}}, t)\, dt$$

are determined by a solution to Euler's equation

$$\frac{d}{dt}\left(\frac{\partial \mathbf{g}}{\partial \dot{\mathbf{x}}}\right) - \frac{\partial \mathbf{g}}{\partial \mathbf{x}} = \mathbf{0}.$$

Given the optimal trajectory, the forces and moments are related to the wing kinematics by

$$\psi_2 = \sin^{-1}\left(\frac{2x_{2/1}\sin(A_\phi/2)}{A_\phi y_{3/2}} - \frac{2\mathcal{M}_y^a \sin(A_\phi/2)}{A_\phi y_{3/2}\mathcal{F}_z^a}\right) \tag{3.47}$$

$$\theta_2 = \tan^{-1}\left(\frac{\mathcal{F}_x^a}{\mathcal{F}_z^a \cos\psi_2}\right) \tag{3.48}$$

$$\Phi_w = -\frac{\mathcal{F}_z^a}{2qf_\phi \sin(A_\phi/2)\cos\theta_2}, \tag{3.49}$$

where $\mathcal{F}_x^a \neq 0$.

Since the forces are considered independent, the minimization of F_x, F_z, M_y can be performed independently. The functions to be minimized are

$$J_x = \int_{t_0}^{t_f} (F_x/m)^2\, dt \tag{3.50}$$

$$J_z = \int_{t_0}^{t_f} (F_z/m)^2\, dt \tag{3.51}$$

$$J_m = \int_{t_0}^{t_f} (M_y/I_y)^2\, dt. \tag{3.52}$$

The application of Euler's equation results in $\ddot{x}$, $\ddot{z}$, and $\ddot{\theta}$ being constant. With the conditions $x(0) = y(0) = \theta(0) = 0$, and $\dot{x}(t_f) = \dot{z}(t_f) = \dot{\theta} = 0$, it follows that the optimal trajectories are given by

$$\frac{x(t)}{x_f} = -\frac{1}{4}\left(\frac{\dot{x}_0}{x_f}\right)^2 t^2 + \left(\frac{\dot{x}_0}{x_f}\right) t, \tag{3.53}$$

$$\frac{z(t)}{z_f} = -\frac{1}{4}\left(\frac{\dot{z}_0}{z_f}\right)^2 t^2 + \left(\frac{\dot{z}_0}{z_f}\right) t, \tag{3.54}$$

$$\frac{\theta(t)}{\theta_f} = -\frac{1}{4}\left(\frac{\dot{\theta}_0}{\theta_f}\right)^2 t^2 + \left(\frac{\dot{\theta}_0}{\theta_f}\right) t, \tag{3.55}$$

where $x_f := x(t_f)$, $\dot{x}_0 := \dot{x}(0)$, etc. Each of the trajectories is coupled by the ending time per

$$t_f = \frac{2x_f}{\dot{x}_0} = \frac{2z_f}{\dot{z}_0} = \frac{2\theta_f}{\dot{\theta}_0}. \tag{3.56}$$

Hence, the trajectories can also be written

$$x(t) = -x_f(\tau^2 - 2\tau) \tag{3.57}$$

$$x(t) = -z_f(\tau^2 - 2\tau) \tag{3.58}$$

$$\theta(t) = -\theta_f(\tau^2 - 2\tau), \tag{3.59}$$

where $\tau := t/t_f$. The planar trajectory can also be expressed in the form

$$z(x) = \frac{\dot{z}_0}{\dot{x}_0} x, \tag{3.60}$$

which indicates a linear path. The path is either ascending or descending depending on the sign of $\dot{z}_0$. The corresponding forces required for this trajectory are

$$F_x = -\frac{1}{2} m \frac{\dot{x}_0^2}{x_f} = -2m\frac{x_f}{t_f^2} \tag{3.61}$$

$$F_z = -\frac{1}{2} m \frac{\dot{z}_0^2}{z_f} + mg = -2m\frac{z_f}{t_f^2} + mg \tag{3.62}$$

$$M_y = -\frac{1}{2} I_y \frac{\dot{\theta}_0^2}{\theta_f} = -2I_y \frac{\theta_f}{t_f^2}. \tag{3.63}$$

The required inertial forces and moment are thus constant. The fixed body frame forces are found by Eqs. (3.44-3.46).

The forces and moment required to produce the optimal trajectory is substantially dependent on the ratios $\dot{x}_0/x_f$ and $\dot{z}_0/z_f$. Recall, that an important approximation in deriving the aerodynamic forces and moment is that $|\dot{x}(t)|$ and $|\dot{z}(t)|$ are "small" relative to the wing motion. The wing kinematics required to produce these forces can be computed by Eqs. (3.46-48).

4 Landing control.

The flight control problem for flapping wing MAV's has been addressed in several works [10]. Since the flapping motion of the wings The consensus approach. This section details control methods that are suited for the attachment landing problem. These techniques are applied in the numerical example of Sec. 5. Since the longitudinal dynamics are significantly nonlinear, due to multiplicative and trigonometric terms, the focus here is on methods of nonlinear control.

4.1 Control model.

To construct a state-space model of the dynamics, define the state vector

$$\mathbf{x} = \begin{bmatrix} x & z & \theta & U & W & Q \end{bmatrix}^T,$$

and the control vector

$$\mathbf{u} = \begin{bmatrix} \theta_2 & \psi_2 & \Phi_w \end{bmatrix}^T. \tag{4.1}$$

Noting the inertial position dynamics

$$\dot{x} = U\cos\theta - W\sin\theta \tag{4.2}$$
$$\dot{z} = -U\sin\theta - W\cos\theta \tag{4.3}$$
$$\dot{\theta}_1 = -Q, \tag{4.4}$$

the average state dynamics (cf. Sec. 4.2) are of the form

$$\dot{\mathbf{x}}(t) = \boldsymbol{f}(\mathbf{x}) + \boldsymbol{g}(\mathbf{u}), \tag{4.5}$$

where

$$\boldsymbol{f}(\mathbf{x}) = \begin{bmatrix} U\cos\theta_1 - W\sin\theta_1 \\ -U\sin\theta_1 - W\cos\theta_1 \\ -Q \\ -WQ/m - g\sin\theta_1 \\ UQ/m + g\cos\theta_1 \\ 0 \end{bmatrix}, \tag{4.6}$$

and

$$\boldsymbol{g}(\mathbf{u}) = \begin{bmatrix} 0 & 0 & 0 & \mathcal{F}_x/m & \mathcal{F}_z/m & \mathcal{M}_y/I_y \end{bmatrix}. \tag{4.7}$$

From Eqs. (3.24-26), the forces and moment are related to the control input by

$$\begin{aligned} \mathcal{F}_x &= -2qf_\phi \sin(A_\phi/2)\sin\theta_2\cos\psi_2\Phi_w \\ \mathcal{F}_x &= -2qf_\phi \sin(A_\phi/2)\sin\theta_2\cos\psi_2\Phi_w \\ \mathcal{M}_y &= 2qf_\phi \left[x_{2/1}\sin(A_\phi/2) - 0.5A_\phi y_{3/2}\sin\psi_2\right] c\theta_2\Phi_w. \end{aligned}$$

To produce a linear form of the model, let

$$\Delta\mathbf{x} = \mathbf{x} - \mathbf{x}_0 \tag{4.8}$$
$$\Delta\mathbf{u} = \mathbf{u} - \mathbf{u}_0 \tag{4.9}$$

where $\mathbf{x}_0$ is an equilibrium point of Eq. (4.5), and $\mathbf{u}_0$ is the corresponding equilibrium control input. The equilibrium points of interest are those of hovering flight, i.e.,

$$\mathbf{x}_0 = \begin{bmatrix} 0 & 0 & \theta_1^0 & 0 & 0 & 0 \end{bmatrix}^T \tag{4.10}$$
$$\mathbf{u}_0 = \begin{bmatrix} \theta_2^0 & \psi_2^0 & \Phi_w^0 \end{bmatrix}^T. \tag{4.11}$$

The linearized dynamics are then

$$\Delta\dot{\mathbf{x}}(t) = \mathbf{A}\Delta\mathbf{x}(t) + \mathbf{B}\Delta\mathbf{u}(t) \tag{4.12}$$

where

$$\mathbf{A} = \begin{bmatrix} 0 & 0 & -Us\theta_1^0 - Wc\theta_1^0 & c\theta_1^0 & -s\theta_1^0 & 0 \\ 0 & 0 & -Uc\theta_1^0 + Ws\theta_1^0 & -s\theta_1^0 & -c\theta_1^0 & 0 \\ 0 & 0 & 0 & 0 & 0 & -1 \\ 0 & 0 & -gc\theta_1^0 & 0 & -Q/m & -W/m \\ 0 & -gs\theta_1^0 & Q/m & 0 & 0 & U/m \\ 0 & 0 & 0 & 0 & 0 & 0 \end{bmatrix}, \tag{4.13}$$

and

$$\mathbf{B} = 2qf_\phi \sin(A_\phi/2) \begin{bmatrix} 0 & 0 & 0 & 0 & 0 & 0 \\ 0 & 0 & 0 & 0 & 0 & 0 \\ 0 & 0 & 0 & 0 & 0 & 0 \\ 0 & 0 & 0 & b_{44} & b_{45} & b_{46} \\ 0 & 0 & 0 & b_{54} & b_{55} & b_{56} \\ 0 & 0 & 0 & b_{64} & b_{65} & b_{66} \end{bmatrix}, \tag{4.14}$$

where

$$\begin{aligned} b_{44} &= -c\theta_2^0 c\psi_2^0 \Phi_w^0/m \\ b_{45} &= s\theta_2^0 s\psi_2^0 \Phi_w^0/m \\ b_{46} &= -s\theta_2^0 c\psi_2^0/m \\ b_{54} &= s\theta_2^0 \Phi_w^0/m \\ b_{55} &= 0 \\ b_{56} &= -c\theta_2^0/m \\ b_{64} &= (0.5A_\phi y_{3/2} s\psi_2^0/\sin(A_\phi/2) - x_{2/1})/I_y \\ b_{65} &= -0.5A_\phi y_{3/2} c\theta_2^0 c\psi_2^0 \Phi_w^0 (\sin(A_\phi/2) I_y) \\ b_{66} &= (0.5A_\phi y_{3/2} s\psi_2^0/\sin(A_\phi/2) - x_{2/1}) c\theta_2^0/I_y. \end{aligned}$$

The linear model if, of course, primarily useful when the states are kept to within a sufficient magnitude of the origin. All of the standard techniques of linear multivariable control are then available for consideration. For the present case, it is necessary that x, z, and θ_1 are varied over a large distance. Extensional linear techniques such as gain scheduling (Rugh, 1990), and simultaneous optimal control (Al-Sunni and Lewis, 1993), are available in these circumstances. Alternatively, under certain conditions on the structure of the equations of motion, several nonlinear techniques are available. The following two sections apply two of these methods, feedback linearization and backstepping, to the flapping control problem.

4.2 Feedback linearization.

Following the standard approach [cite], define the output vector

$$\mathbf{y} = \begin{bmatrix} x & z & \theta_1 \end{bmatrix}^T \tag{4.15}$$

and the control vector

$$\mathcal{F} = \begin{bmatrix} \mathcal{F}_x & \mathcal{F}_z & \mathcal{M}_y \end{bmatrix}^T \tag{4.16}$$

Taking the second derivative of the output results in

$$\begin{aligned} \ddot{x} &= -W\cos\theta(1+Q/m) - 2g\sin\theta_1\cos\theta_1 - U\sin\theta_1(1+Q/m) \\ &\quad + \cos\theta_1\mathcal{F}_x/m - \sin\theta_1\mathcal{F}_z/m \end{aligned} \tag{4.17}$$

$$\begin{aligned} \ddot{z} &= W\sin\theta_1(1+Q/m) + g(\sin^2\theta_1 - \cos^2\theta_1) - U\cos\theta_1(1+Q/m) \\ &\quad - \sin\theta_1\mathcal{F}_x/m - \cos\theta_1\mathcal{F}_z/m \end{aligned} \tag{4.18}$$

$$\ddot{\theta}_1 = -\mathcal{M}_y/I_y. \tag{4.19}$$

This can be expressed in the form

$$\ddot{\mathbf{y}}(t) = \boldsymbol{f}(\mathbf{y}, \dot{\mathbf{y}}) + \mathbf{G}_0(\mathbf{y}, \dot{\mathbf{y}})\mathbf{F},$$

where

$$\boldsymbol{f}(\mathbf{y}, \dot{\mathbf{y}}) = \begin{bmatrix} -W\cos\theta(1+Q/m) - 2g\sin\theta_1\cos\theta_1 - U\sin\theta_1(1+Q/m) \\ W\sin\theta_1(1+Q/m) + g(\sin^2\theta_1 - \cos^2\theta_1) - U\cos\theta_1(1+Q/m) \\ 0 \end{bmatrix} \tag{4.20}$$

$$\mathbf{G}_0(\mathbf{y}, \dot{\mathbf{y}}) = \begin{bmatrix} \cos\theta_1/m & -\sin\theta_1/m & 0 \\ -\sin\theta_1/m & -\cos\theta_1/m & 0 \\ 0 & 0 & -1/I_y \end{bmatrix}. \tag{4.21}$$

Define the tracking error

$$\mathbf{e} = \mathbf{y} - \mathbf{r}, \tag{4.22}$$

where $\mathbf{r}$ is the reference input. The force input is then defined as

$$\mathbf{F} = \mathbf{G}_0^{-1}\left(-\boldsymbol{f} - \mathbf{K}_1\dot{\mathbf{e}}(t) - \mathbf{K}_2\mathbf{e}(t) + \mathbf{K}_3\int_0^t \mathbf{e}(t)\,d\tau + \dot{\mathbf{r}}(t)\right) \tag{4.23}$$

where $\mathbf{K}_1$, $\mathbf{K}_2$, and $\mathbf{K}_3$ are diagonal matrices with positive elements. The error dynamics become

$$\ddot{\mathbf{e}}(t) = -\mathbf{K}_1\dot{\mathbf{e}}(t) - \mathbf{K}_2\mathbf{e}(t) - \mathbf{K}_3\int_0^t \mathbf{e}(t)\,d\tau, \tag{4.24}$$

which are clearly exponentially stable. The control inputs are found by

$$\mathbf{u} = \mathbf{g}_c(\mathbf{F}) \tag{4.25}$$

where by Eqs. (3.47-49)

$$\mathbf{g}_c = \begin{bmatrix} \sin^{-1}\left(\frac{2x_{2/1}\sin(A_\phi/2)}{A_\phi y_{3/2}} - \frac{2\mathcal{M}_y^a\sin(A_\phi/2)}{A_\phi y_{3/2}\mathcal{F}_z^a}\right) \\ \tan^{-1}\left(\frac{\mathcal{F}_x^a}{\mathcal{F}_z^a\cos\psi_2}\right) \\ -\frac{\mathcal{F}_z^a}{2qf_\phi\sin(A_\phi/2)\cos\theta_2} \end{bmatrix}. \tag{4.26}$$

4.3 Backstepping.

The dynamics are divided into two parts:

$$\dot{\boldsymbol{\eta}} = \boldsymbol{f}(\boldsymbol{\eta}) + \mathbf{G}\boldsymbol{\xi} \tag{4.27}$$

$$\dot{\boldsymbol{\xi}} = \boldsymbol{f}_a(\boldsymbol{\eta}, \boldsymbol{\xi}) + \mathbf{G}_a\mathbf{F}, \tag{4.28}$$

where $\boldsymbol{\eta} = (x, z, \theta_1)$ and $\boldsymbol{\xi} = (U, V, Q)$; thus

$$\boldsymbol{f}(\boldsymbol{\eta}) = \begin{bmatrix} 0 & 0 & 0 \end{bmatrix}^T \tag{4.29}$$

$$\boldsymbol{f}_a(\boldsymbol{\eta}) = \begin{bmatrix} (-WQ/m - g\sin\theta_1) & (UQ/m + g\cos\theta_1) & 0 \end{bmatrix}^T \tag{4.30}$$

$$\mathbf{G} = \begin{bmatrix} \cos\theta_1 & -\sin\theta_1 & 0 \\ -\sin\theta_1 & -\cos\theta_1 & 0 \\ 0 & 0 & -1 \end{bmatrix} \tag{4.31}$$

$$\mathbf{G}_a = \begin{bmatrix} 1/m & 0 & 0 \\ 0 & 1/m & 0 \\ 0 & 0 & 1/I_y \end{bmatrix}. \tag{4.32}$$

Define the function

$$\boldsymbol{\phi} = \mathbf{G}^{-1}\left(-\mathbf{K}_1\mathbf{e}(t) - \mathbf{K_2}\int_0^t \mathbf{e}(\tau)\, d\tau\right), \tag{4.33}$$

where $\mathbf{K}_1$ and $\mathbf{K}_2$ are diagonal matrices with positive terms; it is noted that $\mathbf{G}^{-1} = \mathbf{G}$. Also, define the Lyapunov function

$$V = \frac{1}{2}(x^2 + z^2 + \theta_1^2). \tag{4.34}$$

It can be shown (see Sec. 14.4 of [cite]) that the input

$$\mathbf{F} = \mathbf{G}_a^{-1}\left[\frac{\partial\boldsymbol{\phi}}{\partial\boldsymbol{\eta}}(\boldsymbol{f} + \mathbf{G}\boldsymbol{\phi}) - \left(\frac{\partial V}{\partial\boldsymbol{\eta}}\right)^T - \boldsymbol{f}_a - k(\boldsymbol{\xi} - \boldsymbol{\phi})\right] \tag{4.35}$$

exponentially stabilizes the system of Eqs. (4.27,28). As before, the control inputs $\mathbf{u}$ are found from Eqs. (4.25,26).

5 Numerical example.

The preceding sections provide the analytical framework for evaluating the attachment landing requirements and methods of nonlinear control for a flapping wing MAV. The purpose of this section is to demonstrate the application of these results with a numerical example, which is based on the a hypothetical vehicle design, resembling the general planform properties of the bunblebee (Dudley and Ellington, 1990); a dynamic flight analysis based on the parameters of this study was conducted by Sun and Xiong (2005). The baseline design parameters are given in Table 1.

Table 1. Flapping vehicle parameters.

Mass	$m = 175 \times 10^{-6}$ kg
Air density	$\rho = 1.25$kg-m^3
Wing reference area	$S = 53 \times 10^{-6}$ m^2
Moment of inertia	$I_y = 0.213 \times 10^{-8}$ kg-m^2
Flapping amplitude	$A_\phi = 116°$
Flapping frequency	$f_\phi = 155$ Hz
x-distance to wing-root	$x_{2/1} = 3.91$ mm
distance to cop	$y_{3/2} = 7.26$ mm

While, as previously discussed in Sec. 4, the control algorithms are based on the average dynamics, subsequent numerical simulations are conducted using the non-averaged dynamic model. The basic structure of the simulation model is shown in Fig. 2.

5.1 Optimal landing trajectories.

The landing requirements are calculated based on the optimal trajectory analysis of Sec. 3.5. For this example, the landing point is taken to be at $x = 0.1$ and $z = 0.05$ m, and the desired pitch angle is $\theta_1 = -70°$ (note the negative angle denote a pitch angle directed toward the sky, not the ground). Also, the initial angular rotation rate is set to $\dot{\theta}_1^0 = 0.01$ deg/s. The resulting actuation requirements for varying landing times, t_f, are shown in Fig. 3. As expected the actuation requirements increase as the landing time becomes smaller. It is important to note that these trajectories represent open-loop performance based on the averaged dynamics. Thus, while these trajectories are theoretically achievable, it may be difficult to achieve the same performance in feedback control for the non-averaged system.

5.2 Hovering flight.

One of the primary requirements of attachment landing is the ability to hover at a large pitch angle. For example, consider a constant hover angle of $\theta_1 = -70°$, in which case the $\mathbf{A}$ and $\mathbf{B}$ matrices of Eq. (4.13,14) are

$$\mathbf{A} = \begin{bmatrix} 0 & 0 & 0 & 0.3420 & 0.9397 & 0 \\ 0 & 0 & 0 & 0.9397 & -0.3420 & 0 \\ 0 & 0 & 0 & 0 & 0 & -1.0 \\ 0 & 0 & -3.3552 & 0 & 0 & 0 \\ 0 & 0 & 9.2184 & 0 & 0 & 0 \\ 0 & 0 & 0 & 0 & 0 & 0 \end{bmatrix},$$

$$\mathbf{B} = \begin{bmatrix} 0 & 0 & 0 \\ 0 & 0 & 0 \\ 0 & 0 & 0 \\ -2.9922 & 5.5561 \times 10^{-3} & 4.18879 \times 10^{-5} \\ 10.3369 & 0 & -3.9861 \times 10^{-3} \\ 0 & -2.1237 \times 10^{3} & 0 \end{bmatrix}.$$

The eigenvalues of the $\mathbf{A}$ matrix are all zero. This is the case for any hovering equilibrium (although inclusion of a pitch damping term results in a negative real valued eigenvalue). Hence, the open-loop system is unstable, and must be stabilized by feedback.

The demonstrate the the basic hovering performance with classical control techniques, a standard linear quadratic regulator optimal control (LQR) is applied based on the performance index

$$\mathbf{J} = \int_0^t (\Delta \mathbf{x}^T \mathbf{Q} \Delta \mathbf{x} + \Delta \mathbf{u}^T \mathbf{R} \Delta \mathbf{u})\, d\tau. \tag{5.1}$$

After some iteration, the following matrices were chosen:

$$\mathbf{Q} = \text{diag}[1, 1, 0.2, 0, 0, 0], \quad \mathbf{R} = 0.5\mathbf{I}_3. \tag{5.2}$$

Here diag[·] denotes a diagonal matrix, and $\mathbf{I}_3$ is a 3×3 identity matrix. The hovering performance is shown in Figs. 4a,b for an initial pitch angle of $\theta_1 = 0$. The results show that the linear controller achieves a bounded response. The performance can likely improved with some form of integral control. However, the LQR controller was found insufficient for stabilizing the vehicle at even small pitch angles. This is attributable to relatively large values of U, W, and Q, which are assumed small in the linear approximation.

5.3 Landing control.

The landing sequence is divided into two parts: (1) an orientation phase where the pitch angle is brought to a large angle, while attempting to regulate the linear motion; and (2) a terminal landing phase where the pitch angle is kept small and the vehicle is brought forward to its target landing position. The vehicle is initially set at a zero pitch angle and at at distance of 100 mm from its landing target. The desired reference pitch angle for the initial orientation phase is set at 70°. For the following simulations, $x_{2/1}$ is set to zero. This was found to produce the best performance, likely due to the uncoupling between the moment, $\mathcal{M}_y$, and the vertical force $\mathcal{F}_z$.

For the feedback linearization method of Sec. 4.3, the gain matrices of Eq. (4.24) are specified as

$$\begin{aligned}
\mathbf{K}_1 &= \text{diag}[100, 100, 4 \times 10^{-4}] \\
\mathbf{K}_2 &= \text{diag}[20, 20, 0.4] \\
\mathbf{K}_3 &= \text{diag}[10, 10, 0.1].
\end{aligned}$$

These were chosen based on numerous iterations. Generally, it was found that the desired pitching rate must be kept relatively small to maintain a reasonable response of x and z (within 10 mm of the origin). Specifically, for the particular vehicle under consideration, it was found that the inital phase must be in excess of 300 seconds. Alternatively, x and z motions can be tracked relatively quickly. The numerical simulation of the the two-part landing sequence is shown Fig. 5a; the corresponding control input is shown in Fig. 5b. Once a pitch angle of 70° is achieved at approximately 360 seconds, a forward x command of 100 mm is initiated, which is achieved in approximately 5 seconds. The terminal phase of the landing is shown in Fig. 5c.

For the backstepping method of Sec. 4.3, the gain matrices of Eq. (4.32) are specified as

$$\begin{aligned}
\mathbf{K}_1 &= \text{diag}[100, 100, 4 \times 10^{-4}] \\
\mathbf{K}_2 &= \text{diag}[10, 10, 1].
\end{aligned}$$

The two-part landing sequence is shown in Figs. 6a, with corresponding control inputs shown in Fig. 6b.

6 Conclusions.

It was shown that three-degree-of freedom actuation scheme is sufficient for the attachment landing problem. These degrees of freedoms are (i) variation of of down-stroke and up-stroke flapping velocity; (ii) rotation of the wing at its root attachment point; and (iii) wing sweep. The rotation of the wing is especially crucial for hovering at a large pitch angle. Also, a large wing rotation is required when the desired landing trajectory is "fast". Control techniques were studied using a full non-averaged, nonlinear numerical simulation. Methods of linear control were found to be unsuitable for the attachment landing problem; a demonstration of this was shown with a standard LQR method for stabilizing hovering dynamics. The nonlinear methods feedback linearization and backstepping were shown to be suitable for landing control. The application of these methods led to a two part landing sequence, the first part of which is a large pitch rotation. This maneuver was found to be significantly unstable, and could not be performed quickly. The second part of the landing sequence is a forward motion (at a high pitch angle), until wall contact is achieved. This maneuver was found to be significantly more stable, and could be performed with a faster settling time.

7 References

Al-Sunni, F.M. and Lewis, F.L. (1993). Gain scheduling simplification by simultaneous control design. *Journal of Guidance, Control, and Dynamics*, 16:602-603.

Arning, R., Dornier, F., and Sassen, S. (2004). Flight control of micro-aerial vehicles. *AIAA-2004-4911, AIAA Guidance, Navigation, and Control Conference and Exhibit*, Providence, Rhode Island, Aug. 16-19, 2004.

Autumn, K., Buehler, M., Cutkosky, M., Fearing, R., Full, R. J., Goldman, D., Groff, R., Provancher, W., Rizzi, A. A., Sranli, U., Saunders, A., Koditschek, D. E. (2005). Robotics in scansorial environments. *Proceedings of the SPIE*, 5804:291-302.

Bhushan, B., Jung, Y. C. (2006). Micro- and nanoscale characterization of hydrophobic and hydrophilic leaf surfaces. *Nanotechnology*, 17:2758-2772.

Bramwell, A. R. S. (1976). Helicopter dynamics. John Wiley and Sons, Inc.

Borst, A. (1990). How do Flies Land. *BioScience*, 40:292-299.

Deng, X., Schenato, L., and Sastry, S.S. (2006). Flapping flight for biomimetic robotic insects: partII-flight control design. *IEEE Transactions on Robotics*, 22:789-802.

Dickinson, M. H., Lehmann, F. O., and Sane, S. P. (1999). Wing rotation and the aerodynamic basis of insect flight. *Science*,284:1954-1960.

Dudley, R. (2000). Biomechanics of insect flight: form, function, evolution, Princeton University Press.

Dudley, R. and Ellington, C.P. (1990). Mechanics of forward flight in bumblebees. I. Kinetics and morphology. *Journal of Experimental Biology*, 148:19-52.

Gao, H., Wang, X., Yao, H., Gorb, S., and Artz, E. (2004). Mechanics of hierarchical adhesion structures of geckos. *Mechanics of Materials*, 37:275-285.

Geim, A. K., Dubonos, S. V., Grigorieva, I. V., Novoselov, K. S., Zhukov, A. A., Shapoval, S. Y. (2003). Microfabricated adhesive mimicking gecko foot-hair. *Nat Mater*, 2:461-463.

Glassmaker, N. J., Jagota, A., Hui, C. Y., and Kim, J. (2004). Design of biomimetic fibrillar interfaces: making contact. *J R Soc Interface*, 1:23-33.

Hui, C. Y., Glassmaker, N. J., Tang, T. and Jagota, A. (2004). Design of biomimetic fibrillar interfaces: 2. Mechanics of enhanced adhesion. *J R Soc Interface*, 1:35-48.

Jagota, A. and Bennison, S. J. (2002). Mechanics of adhesion through a fibrillar microstructure. *Integr Comp Biol*, 42:1140-1145.

Khalil, H. (2004). Nonlinear Systems. Prentice Hall.

Menon, C., Murphy, M., Sitti, M. (2004). Gecko inspired surface climbing robots. *IEEE International Conference on Robotics Biomimetics*, August 22-26.

Northen, M. T., Turner, K. L. (2005). A batch fabricated biomimetic dry adhesive. *Nanotechnology*, 16:1159-1166.

Rugh, W.J. (1991). Analytical framework for gain-scheduling. *IEEE Control Systems Magazine*, 11:79-84.

Sanders, J.A. (1985). Averaging methods in non-linear dynamical systems. Springer-Verlag.

Sane, S. P., Dickinson, M. H. (2001). The control of flight force by a flapping wing: Lift and drag production. *Journal of Experimental Biology*, 204:2607-2626.

Sane, S. P., Dickinson, M. H. (2002). The aerodynamic effects of wing rotation and a revised quasisteady model of flapping flight. *Journal of Experimental Biology*, 205:1087-1096.

Sane, S. P. (2003). The Aerodynamics of insect flight. *Journal of Experimental Biology*, 206:4191-4208.

Schenato, L. (2003). Analysis and control of flapping flight: from biological to robotic insects. Ph.D. Thesis, University of California at Berkeley, December, 2003.

Schenato, L., Campolo, D., and Sastry, S. (2003). Controllability issues in flapping flight for biomimetic micro aerial vehicles (MAVs). *Proceedings of the 42nd lEEE Conference on Decision and Control*, Maul, Hawaii USA, December, 2003.

Seigler, T.M., Neil, D.A., Bae, J.-S., and Inman, D.J. (2007). Modeling and control of large-scale morphing aircraft. *AIAA Journal of Aircraft*, 44(4):1077-1087.

Sitti, M., (2003). High aspect ratio polymer micro/nano-structure manufacturing using nanoembossing, nanomolding and directed self-assembly. *Proceedings of IEEE/ASME Advanced Mechatronics Conference*, 2:886-890.

Sitti, M., Fearing, R. S. (2003). Synthetic gecko foot-hair for micro/nano structures for future wall-climbing robots. *Proceedings of IEEE International Conference on Robotics and Automation*, 1:1164-1170.

Srinivasan, M. V., Zhang, S., and Chahl, J. S. (2001). Landing strategies in honeybees, and possible applications to autonomous airborne vehicles. *Biol. Bull.* 200:216-221.

Sun, M. and Xiong, Y. (2004). Dynamic flight stability of a hovering bumblebee. *The Journal of Experimental Biology*, 208:447-459.

Yurdumakan, B., Raravikar, N. R., Ajayan, P. M., Dhinojwala, A. (2005). Synthetic gecko foothairs from multiwalled carbon nanotubes. *Chem Comm*, 2005:3799-3801.

8 Appendix - Notation

A *physical vector* $\mathbf{a}$ observed from two reference frames, frame $\mathscr{R}_0$ with orthonormal unit vectors $(\mathbf{i}_0, \mathbf{j}_0, \mathbf{k}_0)$, and $\mathscr{R}_1$ with orthonormal unit vectors $(\mathbf{i}_1, \mathbf{j}_1, \mathbf{k}_1)$, can be expressed as

$$\mathbf{a} = a_x \mathbf{i}_0 + a_y \mathbf{j}_0 + a_z \mathbf{k}_0$$

or

$$\mathbf{a} = a'_x \mathbf{i}_1 + a'_y \mathbf{j}_1 + a'_z \mathbf{k}_1$$

where, in general, $a_x \neq a'_x$, $a_y \neq a'_y$, $a_z \neq a'_z$. We will refer to the axes of frame $\mathscr{R}_i$ by it components x_i, y_i, and z_i.

The matrix representation of the vector $\mathbf{a}$, expressed in the frame $\mathscr{R}_0$, is denoted

$$[\mathbf{a}]_0 = \begin{bmatrix} a_x \\ a_y \\ a_z \end{bmatrix}$$

Similarly, the $\mathscr{R}_1$ frame representation of $\mathbf{a}$ is denoted

$$[\mathbf{a}]_1 = \begin{bmatrix} a'_x \\ a'_y \\ a'_z \end{bmatrix}$$

In general, a symbol representing a matrix will be written without the brackets. However, when it is necessary to identify the matrix as a vector representation, we will use the bracket notation $[\,\cdot\,]_i$ where i denotes the corresponding reference frame. In general, we say that $[\mathbf{a}]_i$ is the $\mathscr{R}_i$ representation of $\mathbf{a}$.

The matrix $[\mathbf{a}]_0$ is converted into the matrix $[\mathbf{a}]_1$ by the operation

$$[\mathbf{a}]_1 = C_{10}[\mathbf{a}]_0$$

where C_{10} is a transformation matrix which coverts vector representations in $\mathscr{R}_0$ into vector representations in $\mathscr{R}_1$. The form of this matrix is dependent on the specific manner in which rotation is parameterized (i.e., Euler angles, Euler parameters, etc.). When dealing with right-handed orthonormal basis vectors, this transformation matrix has the useful property

$$C_{10}^{-1} = C_{10}^T := C_{01}$$

That is, its inverse is equal to its transpose (i.e., it is unitary).

The time derivative of $[\mathbf{a}]_1$ is

$$D_t([\mathbf{a}]_1) = D_t(C_{10})[\mathbf{a}]_0 + C_{10} D_t([\mathbf{a}]_0)$$

where the time derivative is denoted $D_t(\cdot) = d/dt(\cdot)$; similarly, we write $D_{tt}(\cdot) = d^2/dt^2(\cdot)$. Poisson's equation provides the relation

$$D_t(C_{10}) = -[\boldsymbol{\omega}_{1/0}]_1^* C_{10}$$

where $\omega_{1/0}$ is the angular velocity vector that quantifies the rotational motion of $\mathscr{R}_1$ with respect to $\mathscr{R}_0$. The symbol $(*)$ denotes the skew symmetric representation of the vector. That is, if $[\omega_{1/0}]_1 := [P\ Q\ R]^T$ then

$$[\omega_{1/0}]_1^* = \begin{bmatrix} 0 & -R & Q \\ R & 0 & -P \\ -Q & P & 0 \end{bmatrix}$$

Since C_{10} is an orthonormal operator, we also have

$$D_t(C_{01}) = C_{01}[\omega_{1/0}]_1^*$$

Thus, the time derivative becomes of $[\mathbf{a}]_1$ becomes

$$D_t([\mathbf{a}]_1) = -[\omega_{1/0}]_1^* C_{10}[\mathbf{a}]_0 + C_{10}D_t([\mathbf{a}]_0)$$

or

$$D_t([\mathbf{a}]_0) = C_{01}[\omega_{1/0}]_1^*[\mathbf{a}]_1 + C_{01}D_t([\mathbf{a}]_1)$$

The second derivative follows in the same manner.

9 Figures.

Fig. 1. Flapping wing kinematics.

Fig. 2. Simulation model schematic.

Fig. 3. Actuation requirements.

Fig. 4a. LQR hovering control.

Fig. 4b. Actuation inputs for LQR hovering control.

Fig. 5a. Feedback linearization control.

Fig. 5b. Actuation requirements for feedback linearization control.

Fig. 5c. Terminal landing phase for feedback linearization control.

Fig. 6a. Backstepping control.

Fig. 6b. Actuation requirements for backstepping control.

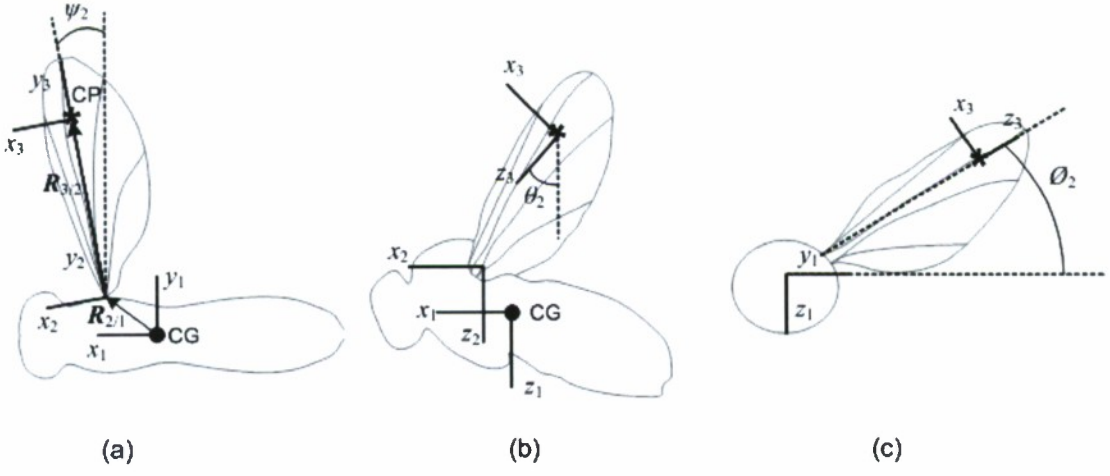

Fig. 1. Flapping wing kinematics.

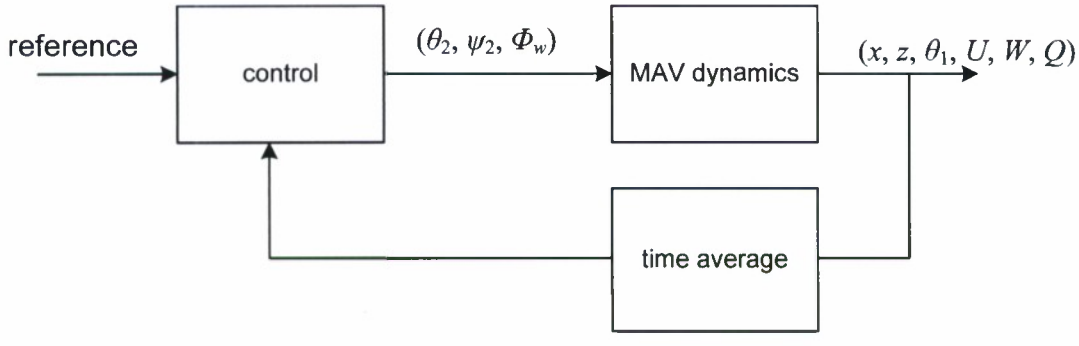

Fig. 2. Simulation model schematic.

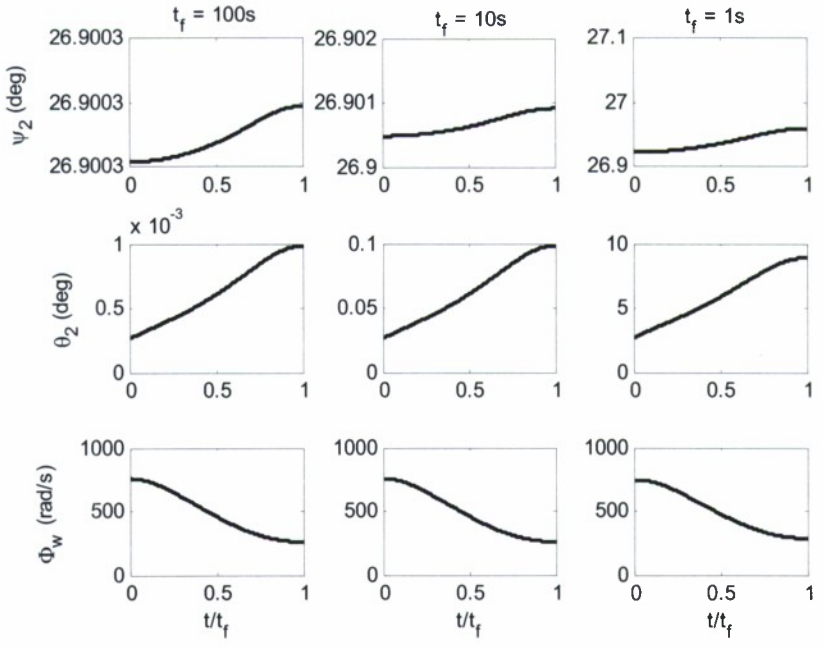

Fig. 3. Actuation requirements.

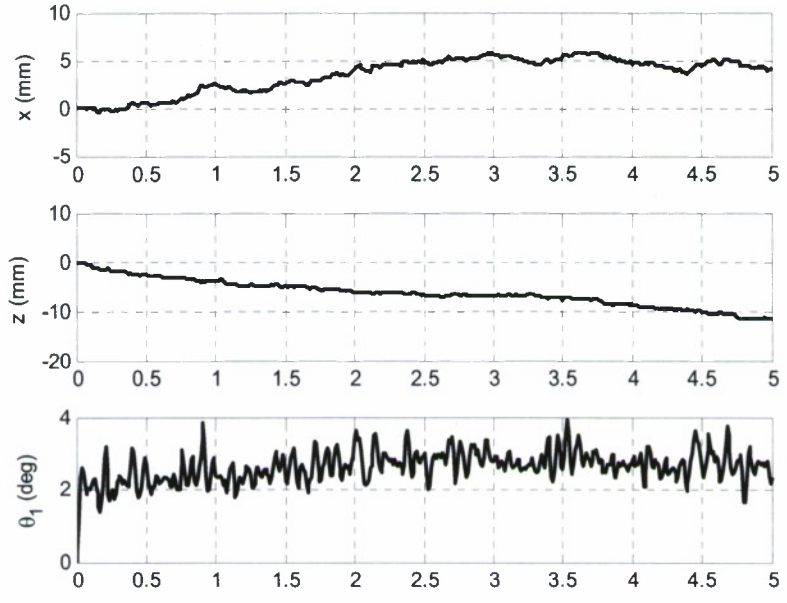

Fig. 4a. LQR hovering control.

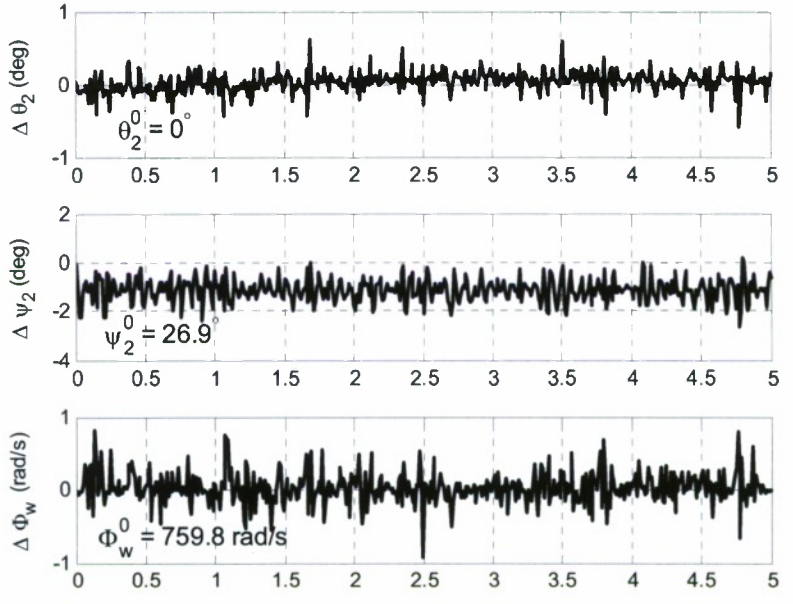

Fig. 4b. Actuation inputs for LQR hovering control.

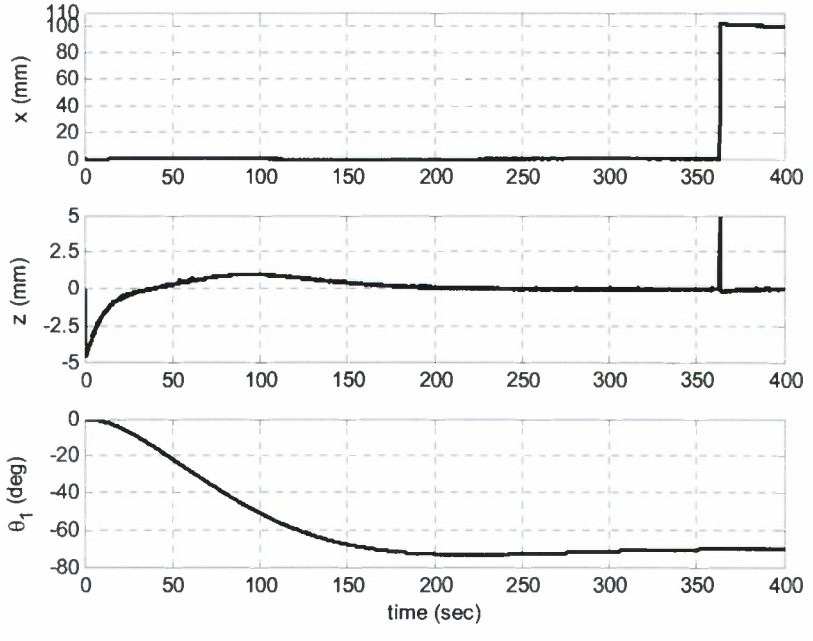

Fig. 5a. Feedback linearization control.

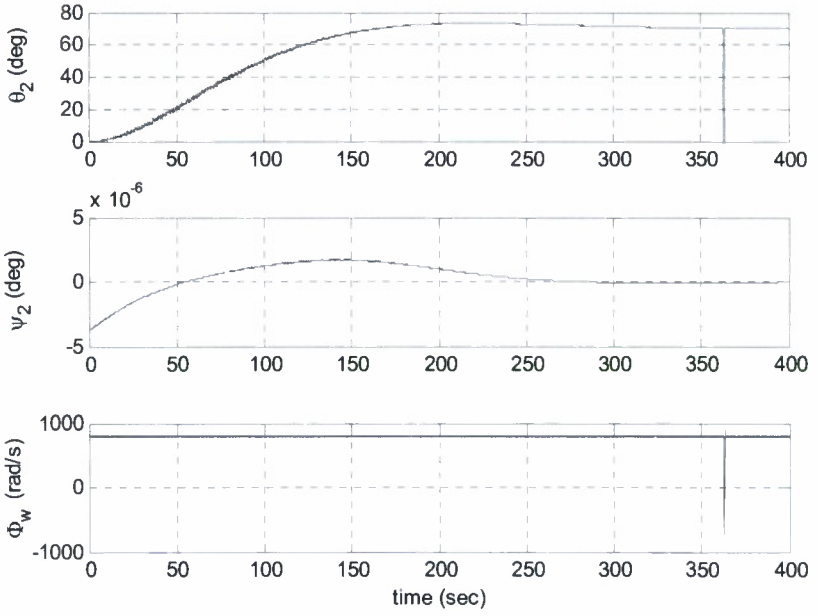

Fig. 5b. Actuation requirements for feedback linearization control.

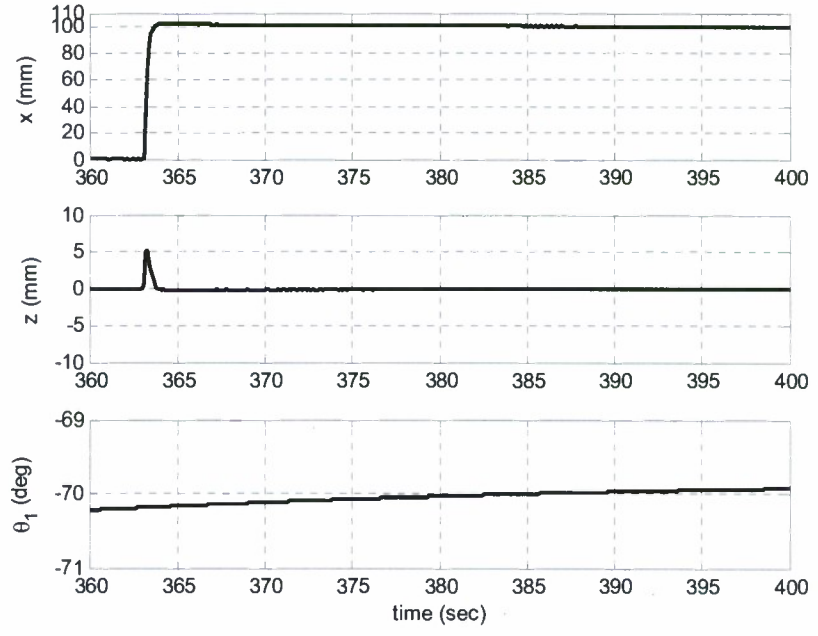

Fig. 5c. Terminal landing phase for feedback linearization control.

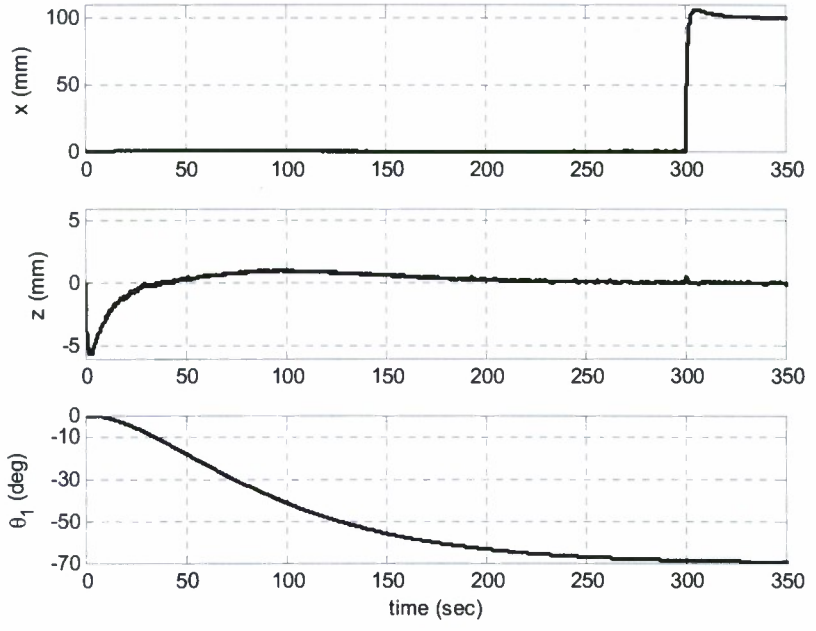

Fig. 6a. Backstepping control.

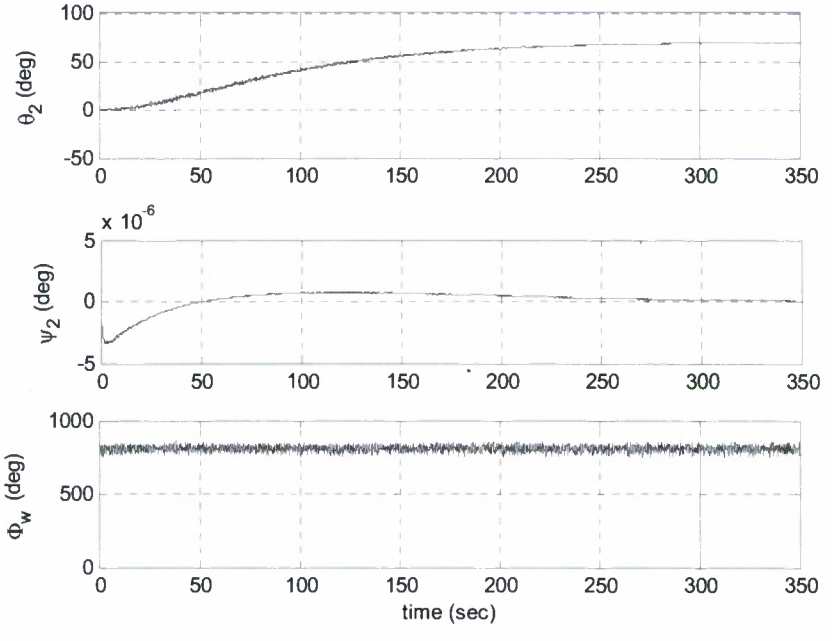

Fig. 6b. Actuation requirements for backstepping control.